Saudi Pharmaceutical Journal 30 (2022) 382–397

Contents lists available at ScienceDirect

Saudi Pharmaceutical Journal

journal homepage: www.sciencedirect.com

Original article

Transdermal permeation of curcumin promoted by choline geranate ionic liquid: Potential for the treatment of skin diseases

Rodrigo Boscariol [a], José M. Oliveira Junior [a], Denicezar A. Baldo [a], Victor M. Balcão [a,b,*], Marta M.D.C. Vila [a,*]

[a] PhageLab – Laboratory of Biofilms and Bacteriophages, University of Sorocaba, 18023-000 Sorocaba, SP, Brazil
[b] Department of Biology and CESAM, University of Aveiro, Campus Universitário de Santiago, P-3810-193 Aveiro, Portugal

ARTICLE INFO

Article history:
Received 4 November 2021
Accepted 29 January 2022
Available online 4 February 2022

Keywords:
Choline geranate ionic liquid
Transdermal permeation
Curcumin
Psoriasis

ABSTRACT

The transdermal permeation of curcumin aided by choline and geranic acid ionic liquid (CAGE-IL) was addressed as a potential treatment for skin diseases. An in-depth analysis of the effect of CAGE-IL concentration in the enhancement of transdermal permeation of curcumin was performed, and the results were modelled via nonlinear regression analysis. The results obtained showed that a low percentage of CAGE-IL (viz. 2.0%, w/w) was effective in disrupting the skin structure in a transient fashion, facilitating the passage of curcumin dissolved in it.

1. Introduction

Curcumin, 7-bis (4-hydroxy-3-methoxyphenyl)-1,6-heptadien-3,5-dione, is a yellow-orange active compound extracted from curcuma rhizomes, especially Curcuma longa L., that exhibits a wide array of biological activities (Carvalho et al., 2015). *Curcuma longa* L. whose scientific synonyms are *C. domestica Valeton* and *Amomum curcuma* Jacq, is a perennial plant belonging to the *Zingiberaceae* family, cultivated in south and southeast tropical Asian countries (Guimarães et al., 2020; Siddiqui, 2015).

Curcumin is a lipophilic compound, whose water solubility at room temperature (both at acidic and neutral pH values) is estimated at 11 ng mL^{-1}. While curcumin is soluble in alkali, it is quite susceptible to self-degradation in this form (Anindya et al., 2015; Stohs et al., 2020). Curcumin is a commercially available mixture of curcuminoids, containing 72–78% of curcumin, 12–18% of demethoxycurcumin, and 3–8% of bisdemethoxycurcumin (Burapan et al., 2020; Hassanzadeh et al., 2020).

The multicomponent nature of curcumin is well documented, possessing "generally recognized as safe" (GRAS) status attributed by the Food and Drug Administration (FDA), and being used as a food additive at different levels between 20 and 500 mg kg^{-1} (EFSA, 2010; Nelson et al., 2017). Clinical reports found in the specialty literature state that curcumin does not produce any harmful effect on the human body even at dosages as high as 1000–2000 mg day^{-1} (Hewlings and Kalman, 2017). However, several adverse effects have been related to the use of curcumin, including gastrointestinal and hematological adverse effects (Agrawal and Goel, 2016).

Curcuma longa has, since ancient times, been widely used in Ayurveda and traditional Chinese medicine for the medical treatment of several diseases (Kocaadam and Şanlier, 2017). In the last few years, numerous scientific studies have rediscovered the therapeutic potential of curcumin and its derivatives due to a wide array of beneficial effects of this compound including (but not limited to) anti-inflammatory, antioxidant, chemoprotective, tissue protective, antibacterial, anti-fungal, antiviral, metabolism regulating, immuno-modulating, antineoplastic and anti-depressant properties (Rendon and Schäkel, 2019; Stohs et al., 2020). In this way, curcumin helps in the recovery from many acute and chronic diseases such as arthritis, diabetes, diabetic microangiopathy, diabetic nephropathy, psoriasis, gastrointestinal diseases, liver disease, inflammation, and others (Burapan et al., 2020; Hassanzadeh et al., 2020; Khalid et al., 2020).

Curcumin has also been reported as having potential for the topical treatment of (but not limited to) diseases such as psoriasis, iatrogenic dermatitis, wounds, and skin cancer (Vollono et al.,

* Corresponding authors at: Universidade de Sorocaba (UNISO), PhageLab, Cidade Universitária Prof. Aldo Vannucchi, Rod. Raposo Tavares km 92.5, CEP 18023-000 Sorocaba/SP, São Paulo, Brazil.
E-mail addresses: victor.balcao@prof.uniso.br (V.M. Balcão), marta.vila@prof.uniso.br (M.M.D.C. Vila).

Peer review under responsibility of King Saud University.

Production and hosting by Elsevier

https://doi.org/10.1016/j.jsps.2022.01.023
1319-0164/

2019). However, due to its intrinsic low solubility in water, many efforts have been made aiming at increasing bioavailability in medicines for topical or systemic use. Research works have been performed employing combination of curcumin with cutaneous permeation facilitators, and encapsulation of curcumin in liposomes, micelles and nanoparticles (Jantarat et al., 2018; Nikolic et al., 2020; Vollono et al., 2019).

Among skin permeation facilitators, ionic liquids (ILs) and their deep eutectic solvents (DESs) have emerged as promising substances that effectively enhance transdermal permeation (Zakrewsky et al., 2014; Harada et al., 2018). ILs are able to solubilize amphipathic molecules and, therefore, act as perfect solvents for topical and transdermal delivery of bioactive substances. The IL molecules are hypothesized to slip through and around the fat-soluble molecules that make up skin cells, corneocytes, creating small transient openings through which bioactive macromolecules (carried by IL) can permeate (Boscariol et al., 2021). ILs and their DESs are able to transiently disrupt the skin barrier function by modifying the regular arrangement of the corneocytes of the stratum corneum (Islam et al., 2020; Boscariol et al., 2021). Choline and geranic acid ionic liquid (CAGE-IL) has been successfully used by our research group to increase skin permeation of several substances, such as insulin (Jorge et al., 2020), phage particles (Campos et al., 2020; Silva et al., 2021) and curcumin (Boscariol et al., 2021), and also by other research groups (Banerjee et al., 2017).

There is no uniformity in toxic activities exhibited by ILs. The cytotoxicity of ILs depends on their structure and varies widely, from micromolar to millimolar ranges (Egorova et al., 2017). According Musiał et al. (2021) two main factors that influence the cytotoxicity are the type of anion and the length of the alkyl chain substituent to the ion. Cytotoxicity increases with increasing alkyl chain length of the cation due to the ability of the longer alkyl chain to more easily embed in and ultimately disrupt, the cell membrane (Yoo et al., 2016). ILs with longer alkyl chains (n > 4) are more lipophilic than those with shorter alkyl chains. It can be assumed that the former tends to incorporate into the phospholipid bilayers of biological membranes (Musiał et al., 2021). In particular, liquid ionic choline generate has been shown to be safe to use as a skin enhancer. Compared to conventional chemical penetration enhancers such as ethanol, these compounds showed lesser toxicity to cells thereby mitigating the issue of skin irritation that is characteristic of many chemical enhancers (Banerjee et al., 2017). Other works have also demonstrated the effectiveness of CAGE-IL as antimicrobial agents in products for topical use and in higher concentrations. Its efficiency and safety have been demonstrated in human studies indicating its non-toxicity (Shevachman et al., 2020; Ko et al., 2021).

For the delivery of bioactive molecules into the dermis, one can employ gels and hydrogels, using natural biopolymers. Polysaccharide-based hydrogels have received special attention over the last few years, due to their biocompatibility, similarity to the native extracellular matrix, low toxicity and susceptibility to biodegradation by human enzymes. In addition, polysaccharide-based hydrogels can be physically cross-linked, without involving any toxic substances, which makes them attractive in the development of delivery systems for bioactive molecules (Pasqui et al., 2012; Zhu et al., 2019). A biopolysaccharide used with success is locust bean gum (LBG) (Dionísio and Grenha, 2012). LBG is a vegetable galactomannan extracted from locust bean seeds (from the carob tree, *Ceratonia siliqua*), used as a biomaterial in several areas of application such as medical, food and cosmetic, since it allows formation of barriers against water vapors and enhances mechanical properties (Pettinelli et al., 2020). For these reasons, the major goal of the research effort entertained herein was to develop and evaluate a LBG gel integrating CAGE-IL aiming at the delivery of curcumin via transdermal permeation, with potential application in the treatment of skin diseases such as psoriasis.

2. Materials and methods

2.1. Materials

2.1.1. Cell lineages

The HaCaT (immortalized human keratinocytes) cell line used in the cytotoxicity assays was purchased from Sigma-Aldrich (St. Louis, MO, USA). The cells were maintained at 37 °C according to the procedure described by Rocha et al. (2017).

2.1.2. Porcine ear skin

Domestic pig ears were obtained from a local butchery in the region of Sorocaba (São Paulo, Brazil) and, from these, the skin was excised and used in the transdermal permeation assays.

2.1.3. Chemicals

Water was purified in a Master System All (model MS2000, Gehaka, São Paulo, Brazil) to a final resistivity of ca. 18.18 MΩ. cm and conductivity of 0.05 $\mu S \cdot cm^{-1}$. Geranic acid (85% stabilized; ref. W412101-1KG-K), choline bicarbonate (ref. C7519-500ML), locust bean gum (Ref. No. G0753), xanthan gum (Ref. No. G1253), carrageenan gum (Ref. No. C1013), gellan gum (Ref. No. G1910) and curcumin (Ref. No. C1386) were purchased from Sigma-Aldrich (St. Louis, MO, USA). HPLC-grade methanol (LiChrosolv®, CAS-No: 67-56-1) was purchased from Merck (Darmstadt, Germany).

2.2. Experimental procedures

2.2.1. Synthesis of choline and geranic acid ionic liquid (CAGE-IL)

CAGE-IL was prepared according to the procedure described by Jorge et al. (2020), Silva et al. (2021) and Zakrewsky et al, (2014). To a 1000-mL round bottom flask, 48 mL of acid geranic (CAS No. 459-80-3; Sigma-Aldrich, St. Louis MO, USA), 20 mL of choline bicarbonate at 80% (w/v) (CAS No. 62-49-7; Sigma-Aldrich, St. Louis MO, USA) and 20 mL of methanol (CAS No. 67-56-1; Chenco, Brazil) were added. The mixture was magnetically stirred at room temperature, in an open system fashion, overnight, until CO_2 production ceased. The solvent was subsequently removed using a rotary evaporator (BUCHI Labortechnik AG model R-215, Germany), at 60 °C, during ca. 20 min. The CAGE-IL prepared was transferred into a 50 mL Falcon tube, the headspace flushed with nitrogen, and the tube immediately capped and duly sealed with Parafilm™ (Bemis Flexible Packaging, Neenah WI, U.S.A).

2.2.2. Preparation and characterization of biopolysaccharide gels

Biopolysaccharide gel with curcumin. Gel formulations integrating curcumin were prepared using locust bean gum (Ref. No. G0753; Sigma-Aldrich, St. Louis MO, USA), xanthan gum (Ref. No. G1253; Sigma-Aldrich, St. Louis MO, USA), carrageenan gum (Ref. No. C1013; Sigma-Aldrich, St. Louis MO, USA), and gellan gum (Ref. No. G1910; Sigma- Aldrich, St. Louis MO, USA) as gelling agents. For each gel, exact amounts of curcumin (Ref. No. C1386; Sigma-Aldrich, St. Louis MO, USA) (viz. 1.0, 1.5 and 2.0% (w/w)), methylparaben (0.1%, w/w) and gum (2%, w/w) were dispersed in ultrapure water and mixed under continuous magnetic stirring. The resulting gels were evaluated in order to define the best gum to be used with curcumin and CAGE-IL.

Biopolysaccharide gel with curcumin and CAGE-IL. Exact mass concentrations of curcumin (1.0%, 1.5% and 2.0% (w/w)) (Ref. No. C1386; Sigma-Aldrich, St. Louis MO, USA), methylparaben

(0.1%, w/w) and locust bean gum (2%, w/w) (Ref. No. G0753; Sigma-Aldrich, St. Louis MO, USA) were dispersed in ultrapure water under continuous magnetic stirring. Three series of biopolysaccharide gels were prepared, with six samples, each of which receiving a different amount of CAGE-IL: in the first series of biopolysaccharide gels containing 1% curcumin, CAGE-IL was added up to final concentratios of 0, 0.5, 1.0, 1.5, 2.0 and 2.5% (w/w). The same procedure was employed for the biopolysaccharide gels integrating curcumin at 1.5% (w/w) and 2.0% (w/w). In the preparation of the gels, careful homogenization was performed in order to avoid air incorporation.

Determination of biopolysaccharide gel spreadability. The effect of the gum type on the spreadability properties of the biopolysaccharide gel was evaluated. The spreadability tests were carried out using a set of glass plates of different dimensions and weights, a circular mold plate made of glass with a central hole (1.2 cm in diameter) and a support plate. The set (support plate, mold plate and glass plate) was placed on top of paper with a millimetric scale. A sample of the biopolysaccharide gel (ca. 2 g) was introduced into the hole in the mold plate and duly leveled with the help of a spatula. The mold plate was removed, and a glass plate of known weight was placed over the sample so as to spread it on the support plate. The diameters covered by the product sample were read on the millimetric scale of the paper and the average diameter was calculated. All determinations were carried out in triplicate at 25 °C. The spreadability (Ei) was then calculated using Eq. (1).

$$E_i = \frac{d^2 \times \pi}{4} \quad (1)$$

where E_i is the spreadability for a given weight of the glass plate (mm^2); d is the mean diameter (mm); and π is the pi number. Plate 1 wt = 162.41 g; Plate 2 wt = 135.26 g; Plate 3 wt = 95.23 g; Plate 4 wt = 61.47 g; Plate 5 wt = 34.65 g; Plate-mold with central orifice = 22.91 g.

Rheological analyses. The viscosity of the gel formulations was studied in a viscometer from Brookfield (model Dv-I Prime, Middleboro MA, U.S.A.). For all gel formulation samples, one used a Brookfield spindle with reference S-28, at rotating speeds of 20, 30, 50, 60, and 100 rpm, at both 25 °C (room temperature) and 33.5 °C (the normal average temperature of the human skin surface). All analyses were carried out in triplicate. The viscometer software provides, in addition to the values of viscosity, results of shear stress as a function of shear rate, and so these results were also used for the rheological characterization of the various gel formulations produced. The shear stress was determined mathematically by using Eq. (2), where τ is the shear stress, γ is the shear rate, and η is the viscosity. The shear stress and shear rate were used to characterize the flow behavior of the various gels.

$$\tau = \gamma \times \eta \quad (2)$$

The thixotropic or rheopectic behavior of the gels was evaluated on the basis of the measurements of viscosity (η) as a function of time (t).

Fourier Transform Infrared spectrophotometry (FTIR) analyses. Sample weights of ca. 2 mg were mixed with 300 mg of KBr so as to form a tablet. The FTIR spectra of samples of pure curcumin (CUR); gel containing 2% (w/w) LBG and 2% (w/w) curcumin; gel containing 2% (w/w) LBG, 2% curcumin (w/w) and 2% (w/w) DES; and gel containing 2% (w/w) LBG, 2.087% (w/w) commercial turmeric (containing 2% (w/w) curcumin) and 2% (w/w) CAGE-IL, were gathered using a Fourier Transform Infrared Spectrophotometer from Shimadzu (model IR-Affinity-1, Shimadzu, Kyoto, Japan), in the wavenumber range from 4000 cm^{-1} to 400 cm^{-1}, with a resolution of 2 cm^{-1}, and using Happ-Genzel apodization.

Mechanical analyses. Mechanical properties (hardness, compressibility, adhesiveness and cohesiveness) of the gel containing 2% (w/w) LBG and 2% (w/w) curcumin; gel containing 2% (w/w) LBG, 2% (w/w) curcumin and 2% (w/w) DES; and gel containing 2% (w/w) LBG, 2.087% (w/w) commercial turmeric (containing 2% (w/w) curcumin) and 2% (w/w) CAGE-IL, were evaluated via relationship between force (N) versus time (s) using a probe (P/10) in a texturometer from Stable Micro Systems (model TA.XT Plus Texture Analyser, Godalming, United Kingdom). Beforehand, the texturometer was calibrated with a load cell with mass of 5 kg. An aliquot of each sample was transferred to a glass beaker and kept in a water bath with temperature adjusted independently to either 25 °C or 33.5 °C. For the temperature of 25 °C, an analytical probe with 10 mm in diameter was compressed on the surface of the samples, with a force of 0.01 N. The procedure for each sample was performed in triplicate. The test speed was set to a rate of 0.5 mm s^{-1}, with a 5% strain mode. The probe's penetration depth was set to 1 mm. For the temperature of 33.5 °C, an analytical probe with a diameter of 10 mm was compressed on the surface of the samples, with a force of 0.005 N. The procedure for each sample was also performed in triplicate. The test speed was set to a rate of 0.5 mm s^{-1}, with a strain mode of 2.5%. The probe's penetration depth was also set to 1 mm.

Evaluation of the cytotoxicity potential of the biopolyssacharide gel integrating both curcumin and CAGE-IL via the agar disk-diffusion assay. The cytotoxicity potential of samples of curcumin and of LBG gel formulations was evaluated via the agar disk-diffusion methodology using cell lineage HaCaT. Cell lineage HaCaT was plated in 50 mm Petri plates, at a concentration of $1.5x10^5$ cells/mL using DMEM culture medium supplemented with bovine fetal serum at 10% (w/w), during a period of 48 h at 37 °C, in an incubation chamber with an atmosphere containing 5% CO_2 (v/v). Subsequently, the liquid medium was discarded and solid "overlay" medium (Eagle medium, 2x concentrated, with agar at 1.8 % (w/w) containing 0.01 % (w/w) neutral red, was added. After solidification, the samples (impregnated in sterile filter paper) were placed in the center of the plates and these were incubated during 24 h at 37 °C, in an environment containing 5% (v/v) CO_2. A disc of sterile atoxic paper was used as negative control whereas a disc of sterile latex was used as positive control, following the same procedure described above. The readings of the inoculated plaques were made macroscopically, where the presence of cytotoxicity was observed by the formation of a clear halo around the sample due to cell lysis surrounding the sample tested (Rogero et al., 2003), corresponding to the dead cells, and microscopically, for the morphological changes of the cells surrounding the sample (Rocha et al., 2017; Pusnik et al. 2016; Jorge et al., 2020; Silva et al., 2021).

2.2.3. Spectrophotometric method for quantification of curcumin

Quantification of curcumin was performed by UV–Vis spectrophotometry at a wavelength of 421 nm, using quartz cuvettes, in a UV–Vis Spectrophotometer from Agilent (model Cary 60 UV–Vis, Santa Clara, CA, USA), following the procedure described by Singh and Avupati (2017) with slight modifications. For the transdermal permeation assays, the calibration curve for quantification of curcumin was prepared using standard solutions of pure curcumin (Ref. No. C1386; Sigma-Aldrich, St. Louis MO, USA) in aqueous PEG 10,000 (Merck, Darmstadt, Germany) at 10% (w/v), at several concentrations in the range 0–25 μg mL^{-1} (Abs_{421nm} = 6.0571x[curcumin, μg mL^{-1}] + 0.0003; r^2 = 0.9983). For the skin retention assays, the calibration curve for quantification of curcumin was prepared using standard solutions of pure curcumin (Ref. No. C1386; Sigma-Aldrich, St. Louis MO, USA) in aqueous ethanol at 50% (v/v), at several concentrations in the range 0–25 μg mL^{-1} (Abs_{421nm} = 1.9121x[curcumin, μg mL^{-1}] + 0.1596; r^2 = 0.9870).

2.2.4. In vitro skin permeation assays

Transdermal permeation of curcumin from the biopolysaccharide gel samples was studied in a DHC-6 T Transdermal System from Logan Instruments Corp. (Somerset NJ, USA), using thawed porcine ear skin discs (0.5 mm thick × 30 mm ϕ_{ext}) as permeation membranes, following the procedure described in detail by Boscariol et al (2021), Jorge et al. (2020) and Campos et al. (2020). The porcine ear skin discs were prepared according to the procedure described by Salerno et al. (2010). The porcine ear skin discs were then clamped on top of the Franz diffusion cell (with a 15 mm ϕ_{ext} central hole, contacting the receptor fluid beneath). On top of these porcine ear skin discs, a cavity with ϕ_{ext} = 30 mm was carefully filled with 2 mL ionic liquid suspension (integrating different volume percentages of CAGE-IL), eliminating any air bubbles. To the receptacle of the Franz diffusion cell (possessing a small cylindrical teflon-coated magnetic stirring bar) beneath the porcine ear skin disc, 8 mL of aqueous solution of polyethylene glycol 10,000 (10%, w/v) (PEG 10000, CAS-No. 25322-68-3, Merck, Darmstadt, Germany) were carefully poured until touching the lower surface of skin, ensuring the absence of air bubbles and stretching the skin so as to minimize the presence of furrows. This compartment was thermosttated at 32 ± 3 °C during 30 min. The ionic liquid suspension was allowed to contact with the upper part of the porcine ear skin discs for a period of 720 min. At predetermined time intervals (viz. 0, 15, 30, 45, 60, 120, 180, 240, 300, 360, 420, 480, 540, 600, 660 and 720 min), 2 mL-samples were withdrawn from the receiving fluid beneath the porcine ear skin disk, and 2-mL of fresh aqueous PEG solution were added so as to reset the volume. Determination of the amount of curcumin in the samples was performed via spectrophotometric readings at 421 nm.

2.2.5. Evaluation of in vitro skin retention of curcumin

Extraction of the curcumin retained in the porcine ear skin discs was based on the methodology described by Sato et al. (2007). After 12 h of *in vitro* permeation, the porcine ear skin discs were removed from the diffusion apparatus and the skin area exposed to the receiving fluid was cleaned with aqueous ethanol (50% (v/v)), and cut and shredded. The skin fragments thus produced were processed with 25 mL of absolute ethanol using an UltraTurrax tissue homogenizer (model LR 5/10 from IKA Werke GmbH & Co. KG, Staufen, Germany) until total tearing of the skin. The resulting suspension was further subjected to sonication via ultrasounds to disrupt the cells, the resulting suspension was filtered into a 50 mL volumetric flask, and the volume made up with aqueous ethanol (50% (v/v)). Determination of the amount of curcumin retained in the porcine ear skin samples was carried out by spectrophotometry as described earlier.

2.2.6. Permeation parameters

The cumulative amount of curcumin permeated through the porcine skin (Q) was calculated using Eq. (3) (Mitragotri et al., 2011; Patel et al., 2009; Sato et al., 2007).

$$Q = \left(C_{measured,t} \times V_r\right) + \sum_{a=0}^{n-1} \times C_a \times V_a \tag{3}$$

where Q (mg) is the cumulative amount of curcumin permeated after 12 h; $C_{measured,\ t}$ is the measured curcumin concentration in the receptor fluid (μg/mL) at time *t* (min); V_r is the volume (mL) of the receiving solution in the diffusion cell; C_a is the concentration (μg/mL) of the sample withdrawn; and V_a is the volume (mL) of the sample withdrawn.

For the mathematical modelling of the experimental (calculated) data, nonlinear fitting of the lognormal distribution (Eq. (4)) to the experimental data was performed using the graphing software GraphPad Prism v. 9.0 (GraphPad Software, San Diego CA, U.S.A.).

$$f(x;\mu,\sigma) = \frac{1}{x\sigma\sqrt{2\pi}} \times exp\left\{\frac{-(\ln x - \mu)^2}{2\sigma^2}\right\}; x > 0 \tag{4}$$

where μ and σ are the average log and the standard deviations of the log, respectively, with the average being given by ($\mu + \sigma^2/2$) and the variance being given by exp ($2\mu + \sigma^2$) (exp (σ^2) − 1).

The total amount of curcumin permeated over 12 h (Q_{12}) was determined by calculating the area under the curve ($AUC_{0\text{-}12}$) in GraphPad Prism 9.0, by fitting Eq. (5).

$$AUC_{0-12} = A \times \sqrt{2\pi} \times ln(GeoSD) \tag{5}$$

where *A* is related to the amplitude and area of the distribution, and *GeoSD* is the geometric standard deviation (dimensionless).

The maximum concentration of curcumin permeated (C_{max}) was also calculated using GraphPad Prism 9.0, through Eq. (6).

$$C_{max} = \frac{A}{GeoMEAN/exp\left(0.5 \times ln(GeoSD)^2\right)} \tag{6}$$

where *A* is the amplitude, *GeoMEAN* is the geometric mean of the data, and *GeoSD* is the geometric standard deviation (dimensionless).

The curcumin flow (μg $mm^{-2}h^{-1}$) through the porcine ear skin matrix area as a function of time (Mitragotri et al., 2011; Arce et al., 2020) was calculated by using Eq. (7).

$$J = \frac{Q}{A \times t} \tag{7}$$

where *J* is the flow (μg/cm^2/hr); *Q* is the permeate quantity (μg); *A* is the porcine ear skin matrix area (cm^2) available for permeation; and *t* is the time (min).

2.2.7. Scanning electron microscopy analyses (SEM)

After lyophilization in a lyophilizer from ThermoFisher (model ModulyOD R23T-659559-RT, Pittsburgh PA, U.S.A.), the morphology of the biopolysaccharide matrix of the optimized gel formulation was observed in a scanning electron microscope (SEM) from JEOL (model JSM-IT200, Tokyo, Japan) working at high-vacuum, equipped with an Energy Dispersive X-ray Spectrometer (EDS) detector also from JEOL (model DRY SD™25 Detector Unit, Tokyo, Japan). Samples of the lyophilized gel were sputter-coated with a Au film (92 Å thickness) via cathodic pulverization on a carbon layer produced by evaporation in a metalizing device also from JEOL (Sputter Coater model DII-29010SCTR Smart Coater, Tokyo, Japan). Photomicrographs were gathered using electron beams with acceleration speeds of 10.0 keV via random scanning.

3. Results

In the research effort described herein, synthesis of choline and geranic acid ionic liquid (CAGE-IL) followed the procedure described in detail by Boscariol et al. (2021), Silva et al. (2021), Jorge et al. (2020), and Zakrewsky et al. (2016), with a product yield of 45% and presenting a density of 1.02 g mL^{-1}, totally fluid and transparent at room temperature. The biopolysaccharide gels produced, integrating both CAGE-IL and either pure or commercial curcumin, were duly characterized and used in transdermal permeation studies of the active principle, aiming at a potential application in the treatment of skin diseases such as psoriasis.

3.1. Determination of biopolysaccharide gel spreadability

The spreadability tests performed to the several biopolysaccharide gels produced indicated that the ones prepared with LBG exhibited the highest spreadabilities (Fig. 1). In addition, LBG showed a good compatibility with curcumin, ease of incorporation and homogenization, allowing to produce uniform gel preparations at all curcumin concentrations tested (Fig. 1). Hence, LBG was chosen as the gelling agent for the subsequent research work.

Regarding the results of the spreadability tests of the gel formulations prepared with LBG, CAGE-IL and curcumin (Fig. 2), one could observe that an increase in the concentration of CAGE-IL resulted in a greater spreadability of the gel, probably due to the establishment of hydrogen bonding between CAGE-IL and the biopolysaccharide and also to the low viscosity of CAGE-IL.

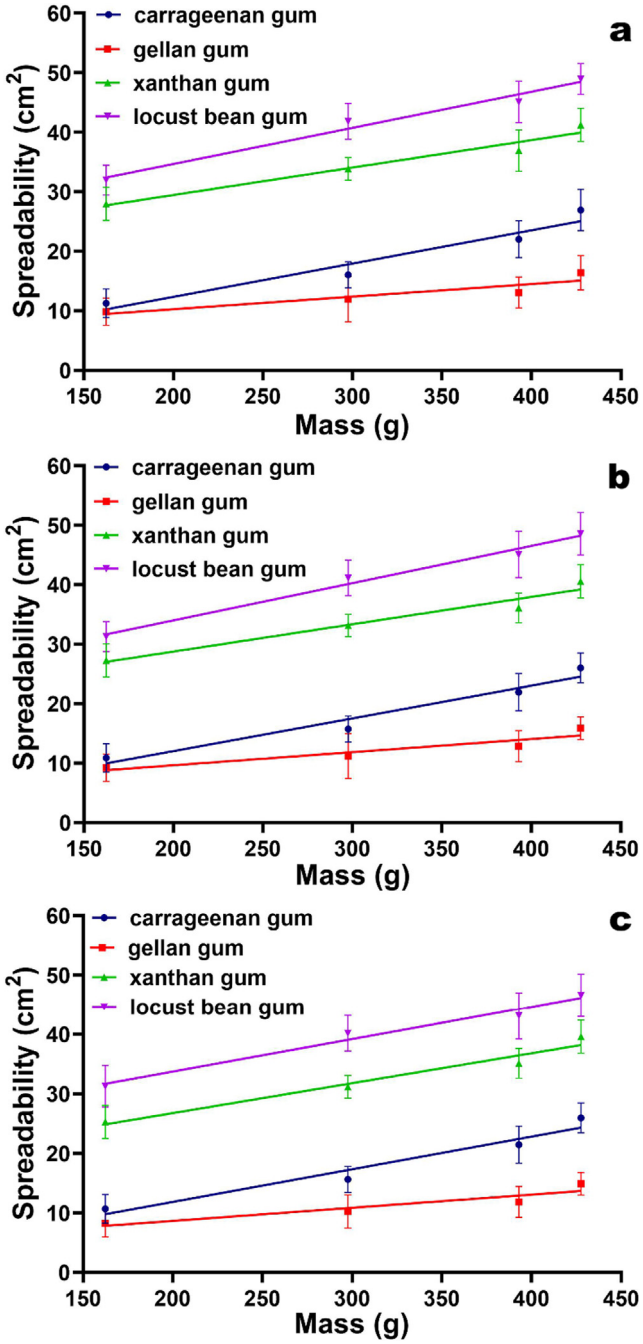

Fig. 1. Spreadability of the gel formulations prepared with the different biopolysaccharide gums and integrating pure curcumin at 1.0% (w/w) (a), 1.5% (w/w) (b) and 2.0% (w/w) (c), as a function of the weight applied. All values represent the mean of three experiments, and the error bars represent the standard deviations.

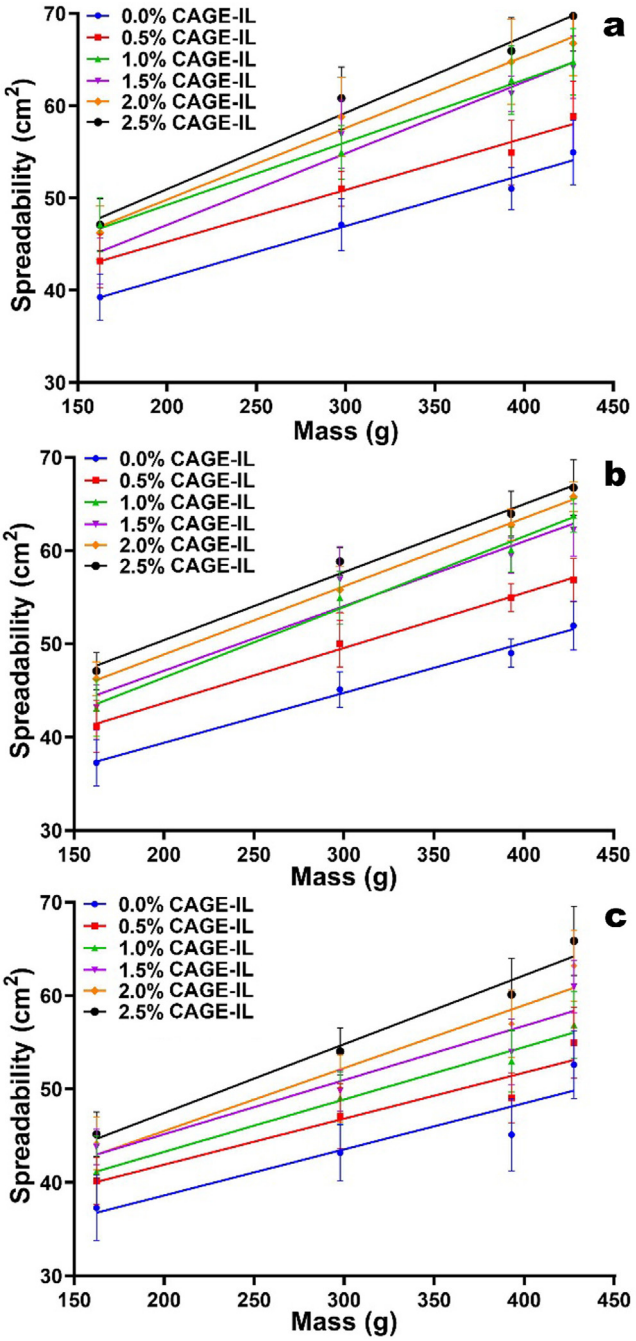

Fig. 2. Spreadability of the gel formulations prepared with LBG and variable concentrations of CAGE-IL, and integrating pure curcumin at 1.0% (w/w) (a), 1.5% (w/w) (b) and 2.0% (w/w) (c), as a function of the weight applied. All values represent the mean of three experiments, and the error bars represent the standard deviations.

3.2. Evaluation of the cytotoxicity potential of the biopolyssacharide gel integrating both curcumin and CAGE-IL via the agar disk-diffusion assay

To carry out these analyzes, the cell line HaCaT (primary mouse embryonic fibroblast cells) was used. The results obtained are displayed in Fig. 3.

3.3. In vitro skin permeation assays

In the IPVT assays carried out in the research effort entertained herein, an aqueous polyethylene glycol (PEG 10000) solution (10%, w/v) was used as the receiving fluid to favor dissolution of the permeated curcumin. Polyethylene glycols are polymers of condensed ethylene oxide, widely used as solvents due to their very high affinity towards water (Zhang et al., 2020).

The results obtained for the cumulative amount of curcumin permeated through the porcine ear skin epidermis, departing from gel formulations integrating different amounts of CAGE-IL, are displayed in Fig. 4.

3.4. Evaluation of in vitro skin retention of curcumin

Determination of the amount of curcumin retained in the porcine ear skin matrix (Fig. 5) following IVPT assays, via UV–Vis spectrophotometry, was performed after ethanol-mediated extraction from the skin matrix. The extraction procedure followed was feasible due to the solubility of curcumin in ethanol (Singh and Avupatil, 2017), without interference of the other components of the porcine ear skin matrix, which were probably also extracted.

3.5. Modelling of in vitro transdermal permeation of curcumin

Most mathematical models postulated for the transport of chemical substances through the *stratum corneum* layer of the skin use one-dimensional diffusion equations, and the popularity of these models lies on their mathematical simplicity. It is assumed that, under steady state conditions, the flow through a permeating membrane is proportional to the concentration gradient across a unit area of a section of the membrane (Mitragotri et al., 2011; Pettinelli et al., 2020).

The transdermal permeation profiles of curcumin integrated in the gel formulations are displayed in Fig. 6, together with non-linear fittings of a lognormal model to the experimental data.

The flow of curcumin permeated through the porcine ear skin as a function of time is displayed in Fig. 7, with a close inspection of the data in this figure allowing to observe that the flow of curcumin increased with increasing concentrations of CAGE-IL in the gel formulations, up to a concentration of CAGE-IL of 2.0% (w/w).

The transdermal permeation behavior of curcumin from commercial turmeric powder is displayed in Fig. 8.

Hence, in this study, in order to evaluate the permeation parameters one determined the cumulative amount of curcumin permeated through an area of porcine ear skin over a 12 h assay ($AUC_{0\text{-}12}$), the flux (J), the maximum time for permeation (t_{max}), and the maximum permeated concentration (C_{max}), for all gel formulations, and the results obtained are displayed in Table 1 for the gel formulation prepared with pure curcumin, and in Table 2 for the gel formulation prepared with raw turmeric, together with the coefficients of determination (r^2).

3.6. Fourier Transform infrared spectrophotometry (FTIR) analyses

Fig. 9 shows the FTIR spectra of pure curcumin, commercial turmeric, gel formulation integrating pure curcumin, gel formulation integrating pure curcumin and CAGE-IL, and gel formulation integrating commercial turmeric and CAGE-IL.

3.7. Rheological analyses

The viscosity of the gel formulations integrating CAGE-IL and either pure curcumin or commercial turmeric are displayed in Fig. 10a for two different temperatures, viz. 25 °C (room temperature) and 33.5 °C (the normal average temperature of the human

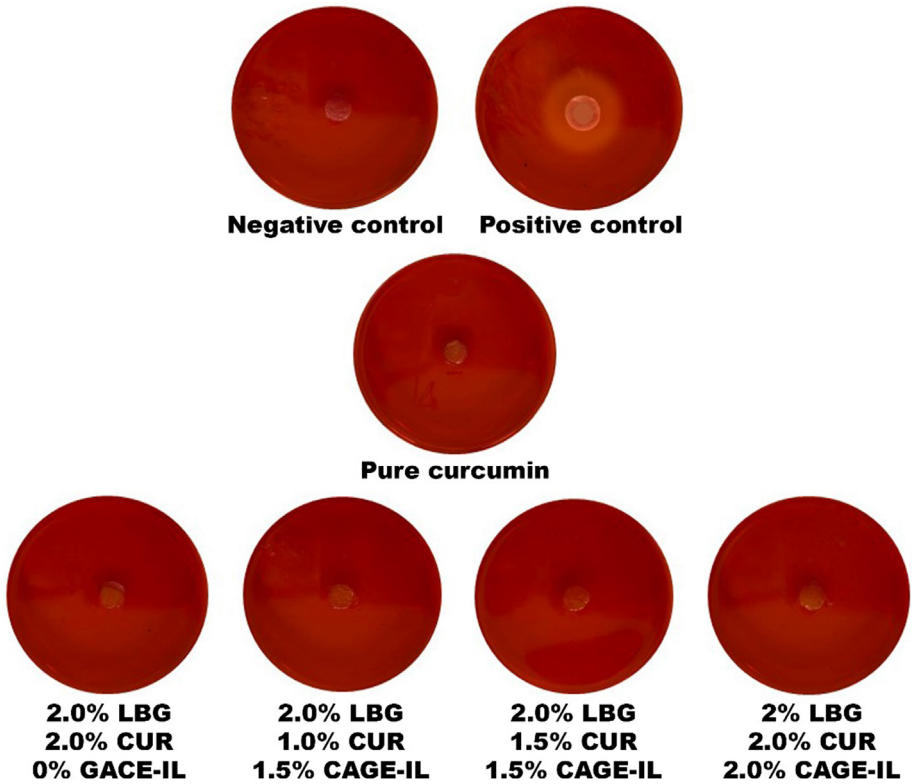

Fig. 3. Results obtained in the analysis of the potential for cytotoxicity via the agar disk-diffusion method with HaCaT cells, of pure curcumin and of the LBG gel gel formulations integrating both curcumin and CAGE-IL at various concentrations.

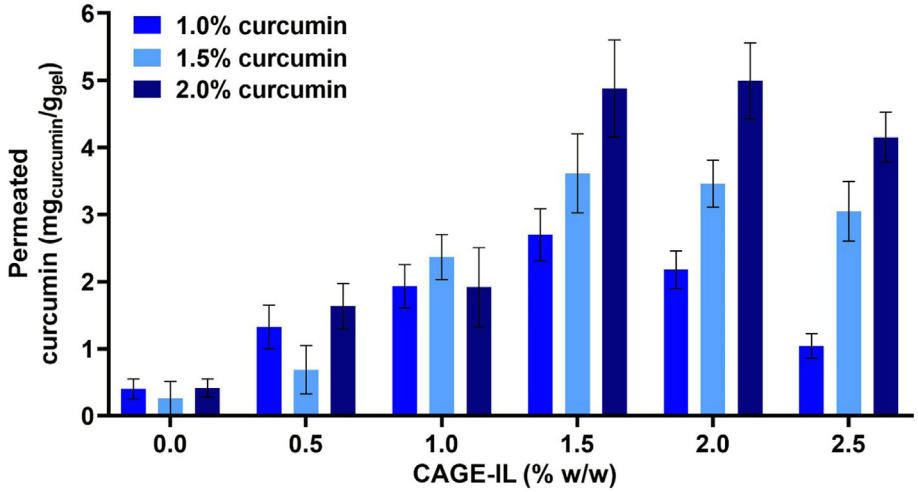

Fig. 4. Net amounts of curcumin permeated from the gel formulations containing different concentrations of curcumin and CAGE-IL. All values represent the mean of three experiments, and the error bars represent the standard deviations.

skin surface), whereas Fig. 10b displays the relationship between shear stress and shear rate allowing to determine the flow behavior of the same gel formulations at the two aforementioned temperatures.

3.8. Mechanical analyses

Evaluation of the mechanical properties of the gel formulations produced integrating pure curcumin with or without CAGE-IL and of the gel formulation integrating commercial turmeric and CAGE-IL, encompassed hardness, compressibility, adhesiveness and cohesiveness, parameters obtained from force-time curves of texture profile analysis (Fig. 11), at two different temperatures, viz. viz. 25 °C (room temperature) and 33.5 °C (the normal average temperature of the human skin surface).

The compressibility, hardness, adhesiveness and cohesiveness of the gel formulations produced integrating pure curcumin with or without CAGE-IL and of the gel formulation integrating commercial turmeric and CAGE-IL, calculated from the force–time curves of texture profile analysis (Fig. 11), are displayed in Fig. 12 for the two different temperatures assayed, viz. 25 °C and 33.5 °C.

The biopolysaccharide matrix of the optimized gel formulation was analyzed via scanning electron microscopy, and photomicrographs of its morphology are displayed in Fig. 13 at different magnifications.

4. Discussion

There is no consensus on the definition of the best concentration of curcumin for topical treatments of skin diseases, with concentrations of curcumin ranging generally from 1% to 2% (w/w) in topical formulations. In this sense, in the research effort entertained herein, biopolysaccharide gels were produced integrating 1.0, 1.5 and 2.0% (w/w) of pure curcumin (Kim and Lio, 2020; Panahi et al., 2019; Vollono et al., 2019). The pharmaceutical form "gel" was therefore used to evaluate the effectiveness of CAGE-IL in enhancing the delivery of curcumin via the transdermal route. Usually, biopolymeric gel formulations are able to retain hydrophobic molecules and thus act as ideal carriers for bioactive molecules aiming at transdermal delivery. In addition, gel formulations are preferred over other topical semisolid preparations, since it has a longer residence time on the skin, higher viscosity, moisturizing effect on flaky skins due to its occlusive properties, higher bio-adhesiveness, promotes less irritation, is independent of the water solubility of the active biomolecule, is easy to apply and exhibits better release characteristics (Aiyalu et al., 2016).

Several natural biopolysaccharide gums were exploited in the study described herein, viz. locust bean gum (LBG), xanthan gum, carrageenan gum and gellan gum, aiming at developing a product with good spreadability and ability to homogeneously integrate curcumin. Besides being cheap, chemically inert, biocompatible, nontoxic, odorless and abounding, natural gums are able to increase the viscosity of a solution even at low concentrations (Mohammadinejad et al., 2020).

Another advantage observed with the use of LBG, when further adding CAGE-IL at several concentrations, was the fact that the gel formulations could be prepared without the need for adding surfactants.

A close inspection of the data in Fig. 2 allows to conclude that spreadability increases in line with the increase in the concentration of CAGE-IL, irrespective of the concentration of curcumin added to the gel.

The results obtained in the cytotoxicity assays showed the non-occurrence of cell death caused by contact with either of the gel formulations containing curcumin (CUR) and CAGE-IL, after 24 h, with the microscopy analyses confirming the integrity of the cells, thus making it possible to observe the clear halo indicative of cell death only for the positive control (in this control, the HaCaT murine cells showed changes in morphology and death (Fig. 3)).

In the evaluation of products for dermatological applications, clinical tests may be preceded, and in some cases replaced by, *in vitro* permeation testing (IVPT). *In vitro* tests allow to understand some of the phenomena that take place between application of the product and its pharmacological effect, in a practical, fast way, and without interference of any biological factors (Pettinelli et al., 2020). In IVPT, the permeation membrane is a critical factor for performing the transdermal permeation experiments. Synthetic membranes do not exhibit the anatomical and physiological features of the human skin, hence the idea is to perform transdermal permeation studies using natural membranes (either human or animal skin). Human skin is definitely the most suitable membrane for IVPT studies (Arce et al., 2020), but unfortunately it is not always accessible. Therefore, the IVPT assays were carried out using porcine ear skin as permeation membrane. Porcine ear skin has been often used as a mimicking alternative to the human skin in studies of percutaneous absorption when developing formula-

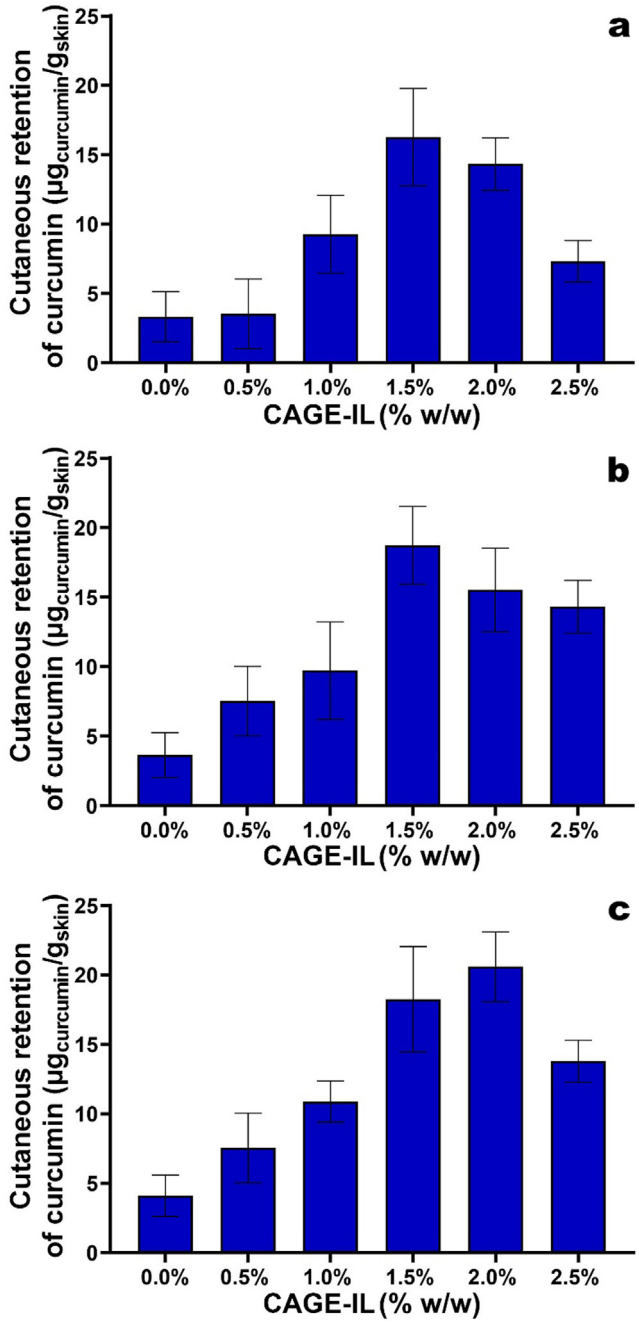

Fig. 5. Results obtained for the average amount of curcumin retained in the porcine ear skin matrix, as a function of the concentration of CAGE-IL for gel formulations integrating pure curcumin at (a) 1.0% (w/w), (b) 1.5% (w/w), and (c) 2.0% (w/w). All values represent the mean of three experiments, and the error bars represent the standard deviations.

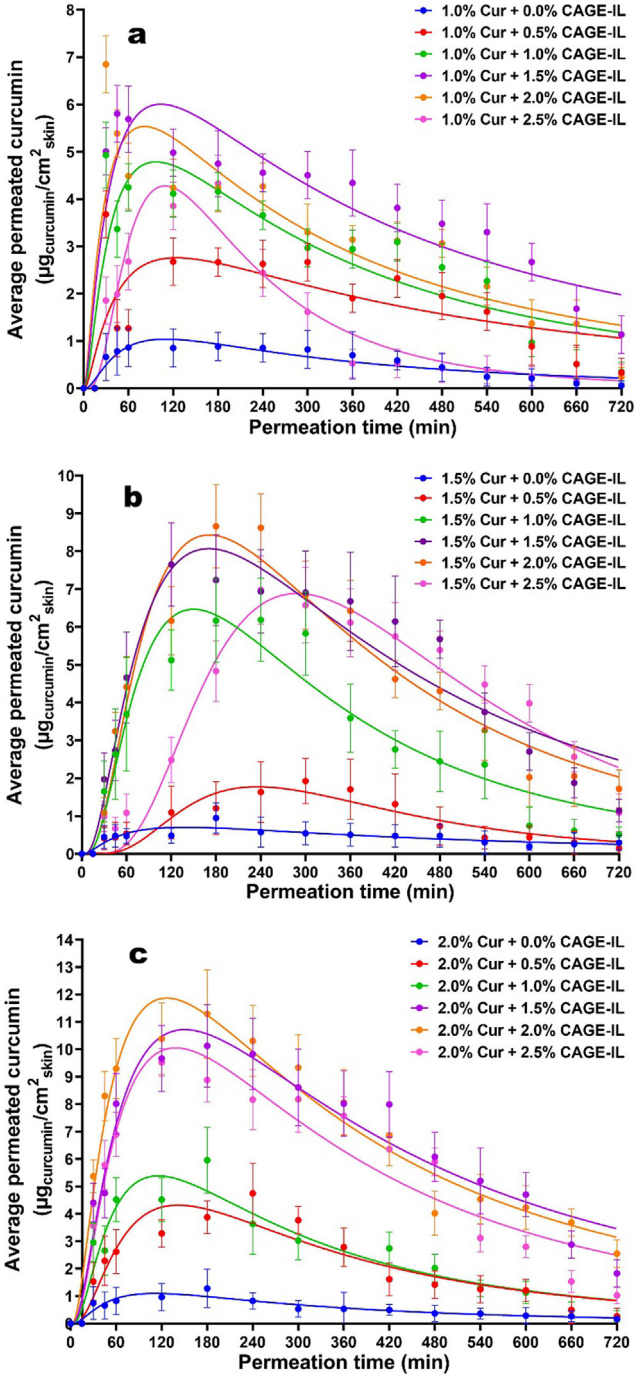

Fig. 6. Time evolution of the *in vitro* skin permeation of curcumin from the gel formulations integrating variable amounts of CAGE-IL and curcumin at (a) 1.0% (w/w), (b) 1.5% (w/w), and (c) 2.0% (w/w). Nonlinear fittings of the lognormal model are depicted by solid lines. All values represent the mean of three experiments, and the error bars represent the standard deviations.

tions for transdermal delivery of bioactive moieties (Boscariol et al., 2021; Silva et al., 2021; Hernandes et al., 2021; Jorge et al., 2020; Campos et al., 2020; Todo, 2017; Zakrewsky et al., 2016). Several *in vitro* studies of transdermal permeation using Franz cells have indicated that porcine ear skin is the one that has flow values and permeation coefficients closest to the human skin (Ahad et al., 2021; Islam et al., 2020).

From inspection of the data in Fig. 4, one may conclude that CAGE-IL enhanced the transdermal permeation of curcumin. As can be observed from inspection of the results in Fig. 4, CAGE-IL at concentrations of 1.5% (w/w) and 2.0% (w/w) promoted the best results in terms of total permeated curcumin for all curcumin concentrations integrated in the gel. At a concentration of 2.5% (w/w), CAGE-IL promotes disruption of the *stratum corneum* and a lower amount of permeated curcumin, probably due to saturation of the skin, a result that is in close agreement with previous reports (Boscariol et al., 2021).

According to Yousef et al. (2019) the mechanism of skin penetration enhancement of curcumin may be due to three different processes. The increase in permeation may be a function of the action of the vehicle, contact surface increase (nanoparticles) and

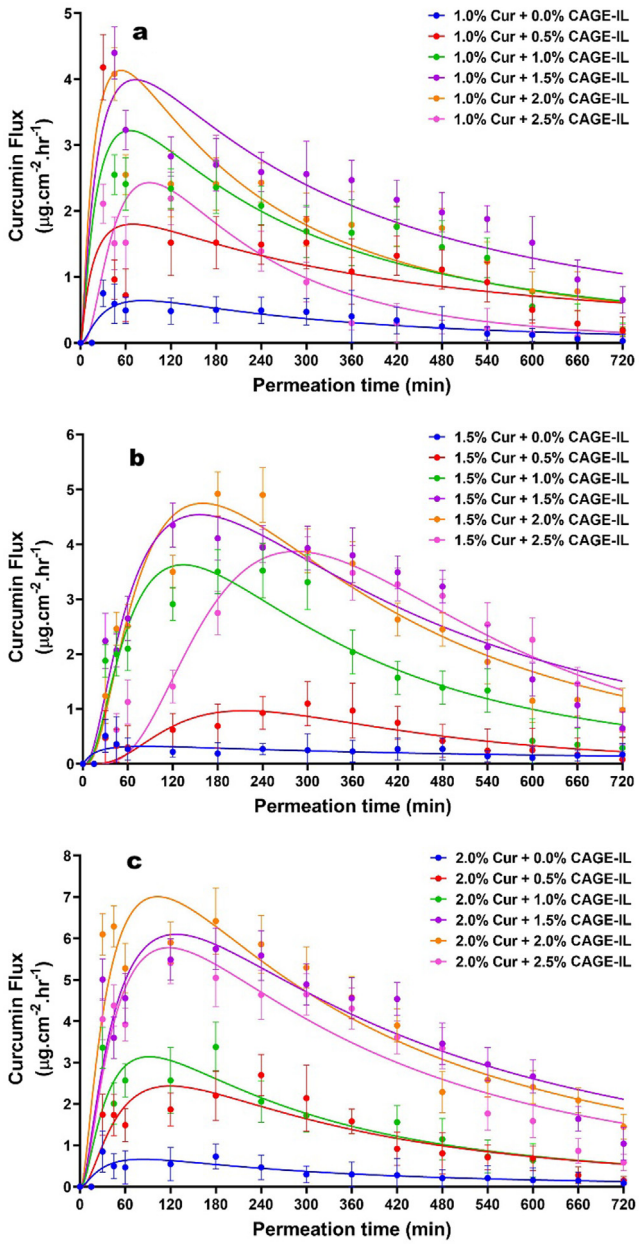

Fig. 7. Time evolution of the *in vitro* skin flow of permeated curcumin from the gel formulations integrating variable amounts of CAGE-IL and curcumin at (a) 1.0% (w/w), (b) 1.5% (w/w), and (c) 2.0% (w/w). Nonlinear fittings of the lognormal model are depicted by solid lines. All values represent the mean of three experiments, and the error bars represent the standard deviations.

by modification of the solvent nature of the stratum corneum caused by fluidisation of the stratum corneum lipids. In the work developed, there may be an increase in permeation due to the greater solubilization of curcumin by the ionic liquid and by momentary changes in the corneal extract.

As can be observed from inspection of the data displayed in Fig. 5, the amount of curcumin retained inside the skin matrix was more significant when CAGE-IL was integrated in the gel formulations at levels equal or higher than 1.5% (w/w), for all curcumin concentrations tested. In the gel formulation containing the highest concentration of curcumin (viz., 2.0% (w/w)) (Fig. 5c), the best result in terms of the amount of curcumin retained within the skin matrix was obtained when CAGE-IL was integrated in the gel at a concentration of 2.0% (w/w). This result is in fact highly significant if this gel formulation is intended for the topical treatment of psoriasis, since this very concentration of CAGE-IL allowed the highest level of transdermal permeation of curcumin (Fig. 4) for the highest level of curcumin integrated in the gel, while allowing saturation of the skin with the highest amount of curcumin (Fig. 5).

Human skin permeability values have previously been identified to follow a log-normal (or skewed non-normal) distribution (Pradal, 2020; Defraeye et al., 2020; LaCount et al., 2020; Chen et al. 2016; Purushothaman et al., 2016; Limpert et al., 2001; Williams et al., 1992), hence favoring the use of geometric means to compare between formulations. The geometric mean is a good proxy to describe permeability, when the spatial distribution of permeability for the (heterogeneous) skin matrix, with no evidence of anisotropy, is lognormal (Selvadurai and Selvadurai, 2014). The generative process leading to a lognormal distribution was explained a long time ago by Gibrat (1930), who named it "law of proportional effect", being closely related to the power law distribution (Mitzenmacher, 2003).

As can be observed from a close inspection of the data displayed in Fig. 6, the time profile of curcumin permeated through the skin in an experimental model *in vitro* was adequately described by the aforementioned non-linear lognormal model.

The transdermal permeation behavior of curcumin was similar for all concentrations of curcumin integrated in the gel formulations (Fig. 6), with an initial higher release being observed during the first 120 min of assay and, after that, a consistent decrease in the amount of permeated curcumin until the end of the assay timeframe, most likely due to skin saturation.

From inspection of the data in Fig. 6 it is clear that for gel formulations containing 1.0% (w/w) and 1.5% (w/w) curcumin, CAGE-IL added at 1.0% (w/w), 1.5% (w/w) and 2.0% (w/w) promoted the highest amounts of permeated curcumin (Fig. 6a and 6b), indicating that the presence of the ionic liquid enhances the transdermal permeation of curcumin, results that are in close agreement with previous findings (Boscariol et al., 2021). Notwithstanding this observation, the gel formulation integrating CAGE-IL at 2.0% (w/w) promoted the highest permeation of curcumin when it was added at 2.0% (w/w) (Fig. 6c), whereas CAGE-IL added at 2.5% (w/w) exhibited lower results for the amount of permeated curcumin. According to Boscariol et al. (2021), Silva et al. (2021), Jorge et al. (2020), and Sidat et al. (2019), ionic liquids and their deep eutectic solvents have, in general, the ability to enhance transdermal permeation of biomacromolecules, employing mechanisms such as disruption of cellular integrity, fluidization, and creation of diffusional pathways (Boscariol et al., 2021), and extraction of lipid components within the *stratum corneum*. In this sense, higher concentrations of CAGE-IL may lead to disruption and flaking of the *stratum corneum*, impairing permeation by altering or disturbing the pathways for active compounds to flow through (Boscariol et al., 2021).

The transport of bio(macro)molecules through the skin, in an *in vitro* permeation study, can be considered as a steady-state process resulting from transient disruption of the *stratum corneum* structure, relating the amount of solute that crosses an area of membrane available for permeation. In fact, the *stratum corneum* behaves like a pseudo-homogeneous membrane, where its properties do not vary significantly with position and time (Mitragotri et al., 2011; Arce et al., 2020).

The highest flow values were obtained during the first 60 min for 1% (w/w) curcumin (Fig. 7a), during the first 150 min for 1.5% (w/w) curcumin (Fig. 7b), and during the first 90 min for 2.0% (w/w) curcumin (Fig. 7c). This occurred with the different concentrations of CAGE-IL in the gel formulations. According to Boscariol et al. (2021) and Kováčik et al. (2020), the flow of drugs and fat-soluble chemicals through the skin increases with the presence of a permeation enhancer, a statement clearly in line with the results obtained in the present research work. The results obtained

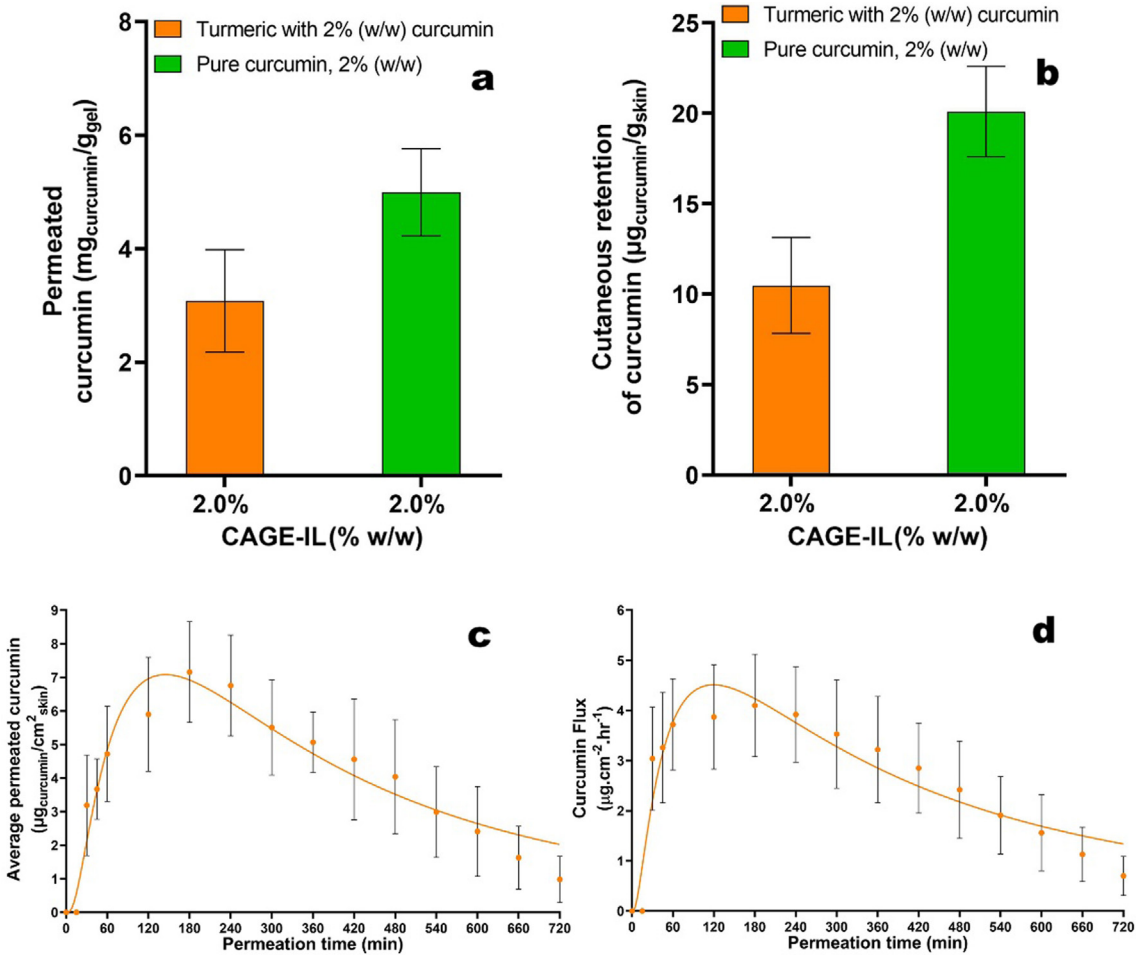

Fig. 8. Total amount of permeated curcumin from the gel formulation integrating commercial turmeric and CAGE-IL (a), average amount of curcumin retained in the porcine ear skin matrix (b), time evolution of the *in vitro* skin permeation of curcumin from the gel formulation integrating commercial turmeric and CAGE-IL (c), time evolution of the *in vitro* skin flow of permeated curcumin from the optimized gel formulation integrating commercial turmeric and CAGE-IL (d). Nonlinear fittings of the lognormal model are depicted by solid lines. All values represent the mean of three experiments, and the error bars represent the standard deviations.

Table 1
Average values of the total amount or curcumin (CUR) permeated in a 12 h assay (AUC_{0-12}), curcumin flux (J) through the skin, time to attain maximum concentration (t_{max}) and maximum concentration attained of permeated curcumin (C_{max}), for the gel formulations integrating curcumin at 1.0 % (w/w), 1.5 % (w/w) and 2.0 % (w/w) and CG-DES at 0 % (w/w), 0.5 % (w/w), 1.0 % (w/w), 1.5 % (w/w), 2.0 % (w/w), and 2.5% (w/w). All values displayed represent the mean of three experiments and associated standard deviations.

CUR (%, w/w)	CG-DES (%, w/w)	AUC_{0-12} (µg)	J (µg·mm^{-2} ·h^{-1})	T_{max} (min)	C_{max} (µg·mL^{-1})	(r^2)
1.0	0.0	398.0 ± 45.5	0.32 ± 0.05	180.0 ± 28.2	0.88 ± 0.20	0.8724
	0.5	1323.0 ± 125.6	1.08 ± 0.14	30.0 ± 7.0	3.68 ± 1.20	0.5065
	1.0	1930.0 ± 322.5	1.64 ± 0.26	30.0 ± 7.0	4.93 ± 1.30	0.7624
	1.5	2695.0 ± 389.2	2.23 ± 0.52	45.0 ± 7.0	5.80 ± 1.20	0.8109
	2.0	2176.0 ± 278.6	1.98 ± 0.36	30.0 ± 7.0	6.84 ± 0.50	0.6946
	2.5	1040.0 ± 185.5	0.87 ± 0.20	180.0 ± 28.0	4.33 ± 0.50	0.9114
1.5	0.0	262.2 ± 55.1	0.21 ± 0.09	45.0 ± 7.0	0.47 ± 0.05	0.6365
	0.5	685.1 ± 360.5	0.46 ± 0.15	300.0 ± 28.0	1.92 ± 0.60	0.8216
	1.0	2368.0 ± 235.7	1.66 ± 0.27	240.0 ± 48.0	6.19 ± 0.55	0.9183
	1.5	3615.0 ± 289.5	2.45 ± 0.65	120.0 ± 48.0	7.65 ± 1.50	0.9598
	2.0	3461.0 ± 350.5	2.33 ± 0.53	180.0 ± 48.0	8.66 ± 1.40	0.9529
	2.5	3048.0 ± 345.4	1.92 ± 0.44	240.0 ± 48.0	6.98 ± 1.60	0.9493
2.0	0.0	412.0 ± 136.4	0.33 ± 0.20	180.0 ± 48.0	1.28 ± 0.35	0.8682
	0.5	1632.0 ± 338.5	1.18 ± 0.50	240.0 ± 28.0	4.75 ± 1.20	0.8672
	1.0	1918.0 ± 289.3	1.48 ± 0.50	180.0 ± 28.0	5.95 ± 1.20	0.8928
	1.5	4880.0 ± 525.1	3.48 ± 0.75	180.0 ± 28.0	10.13 ± 3.20	0.9391
	2.0	4994.0 ± 468.5	3.77 ± 0.87	180.0 ± 48.0	11.30 ± 3.30	0.9499
	2.5	4153.0 ± 372.5	3.01 ± 0.52	120.0 ± 28.0	9.52 ± 2.40	0.9226

Table 2
Average values of the total amount or curcumin (CUR) from commercial turmeric permeated in a 12 h assay (AUC_{0-12}), curcumin flux (J) through the skin, time to attain maximum concentration (t_{max}) and maximum concentration attained of permeated curcumin (C_{max}), for the gel formulations integrating curcumin at 1.0 % (w/w), 1.5 % (w/w) and 2.0 % (w/w) and CG-DES at 0 % (w/w), 0.5 % (w/w), 1.0 % (w/w), 1.5 % (w/w), 2.0 % (w/w), and 2.5% (w/w). All values displayed represent the mean of three experiments and associated standard deviations.

CUR (%, w/w)	CG-DES (%, w/w)	AUC_{0-12} (μg)	J ($\mu g \cdot mm^{-2} \cdot h^{-1}$)	T_{max} (min)	C_{max} ($\mu g \cdot mL^{-1}$)	(r^2)
2.0	2.0	3079.3 ± 603.2	2.45 ± 0.83	160.0 ± 70.0	7.16 ± 1.03	0.9307

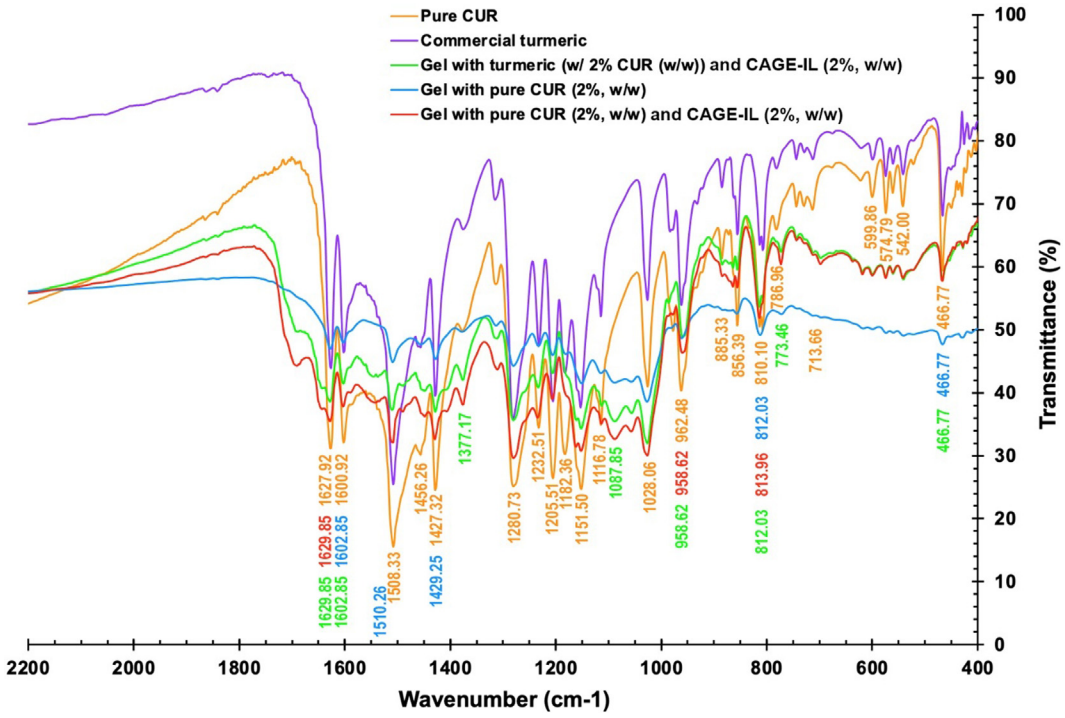

Fig. 9. FTIR spectra of samples of pure curcumin, commercial turmeric, gel formulation integrating pure curcumin, gel formulation integrating pure curcumin and CAGE-IL, and gel formulation integrating commercial turmeric and CAGE-IL.

clearly confirm the efficiency of CAGE-IL as a facilitator for the transdermal permeation of curcumin, when added at concentrations up to 2% (w/w), a result in clear agreement with previous findings (Boscariol et al., 2021).

The transdermal permeation behavior of curcumin from commercial turmeric powder was similar for that of all gel formulations integrating pure curcumin (Fig. 8), but with a lower amount of curcumin being released when employing commercial turmeric, most likely due to interactions between curcumin and other components present in the raw turmeric extract (Fig. 8a).

From inspection of the data in Fig. 8b it is also clear that when employing raw turmeric extract (containing 2.0% (w/w) curcumin) in the gel formulation integrating CAGE-IL at 2.0% (w/w), the amount of curcumin retained in the skin was ca. half of that when using pure curcumin in the gel formulation. Notwithstanding this observation, the gel formulation integrating CAGE-IL at 2.0% (w/w) promoted permeation of curcumin from raw turmeric at acceptable levels and the skin retained more than 10 $\mu g_{curcumin}/g_{skin}$.

The profile of average amount of permeated curcumin from raw turmeric integrated in the gel formulation together with CAGE-IL at 2% (w/w) during the assay timeframe (Fig. 8c) and the flow of curcumin from raw turmeric permeated through the porcine ear skin as a function of time (Fig. 8d) exhibited the same trends as those displayed in Fig. 6 and Fig. 7 for pure curcumin, respectively, allowing to conclude that raw turmeric powder is an economically feasible alternative to pure curcumin when formulating pharmaceutical gel forms aiming at transdermal delivery of this important bioactive molecule with potential in the treatment of skin diseases such as (but not limited to) psoriasis.

A careful inspection of the data displayed in Table 1 allows to conclude that the gel formulations that allowed the highest values for permeated curcumin (viz. AUC_{0-12}, $\mu g_{curcumin}$), curcumin permeation flow (viz. J, $\mu g_{curcumin}$ mm^{-2}_{skin} h^{-1}) and curcumin permeation coefficient (viz. C_{max}, μg mL^{-1}), were those that integrated CAGE-IL at 1.5% (w/w) and 2.0% (w/w) (shaded areas in Table 1).

As the concentration of CAGE-IL in the gel formulation increased from 0% (w/w) to 2.0% (w/w), the transdermal permeation of curcumin was found to increase steadily. However, the use of CAGE-IL at 2.5% (w/w) did not allow an increase in the amount of permeated curcumin compared to the formulations containing CAGE-IL at 2.0% (w/w) (Table 1), with a possible explanation for this observation being that higher concentrations of CAGE-IL may lead to disruption and flaking of the *stratum corneum*, impairing permeation by altering or disturbing the pathways for active compounds to flow through (Boscariol et al., 2021). The results obtained thus suggest that the use of curcumin at 2% (w/w) together with CAGE-IL at 2% (w/w) in the gel formulation promoted the best conditions for a maximum transdermal permeation of curcumin (Table 1). In their studies, Yousef et al. (2019) evaluated the permeation for curcumin from nanoemulsions and concluded that enhanced solubility of curcumin by

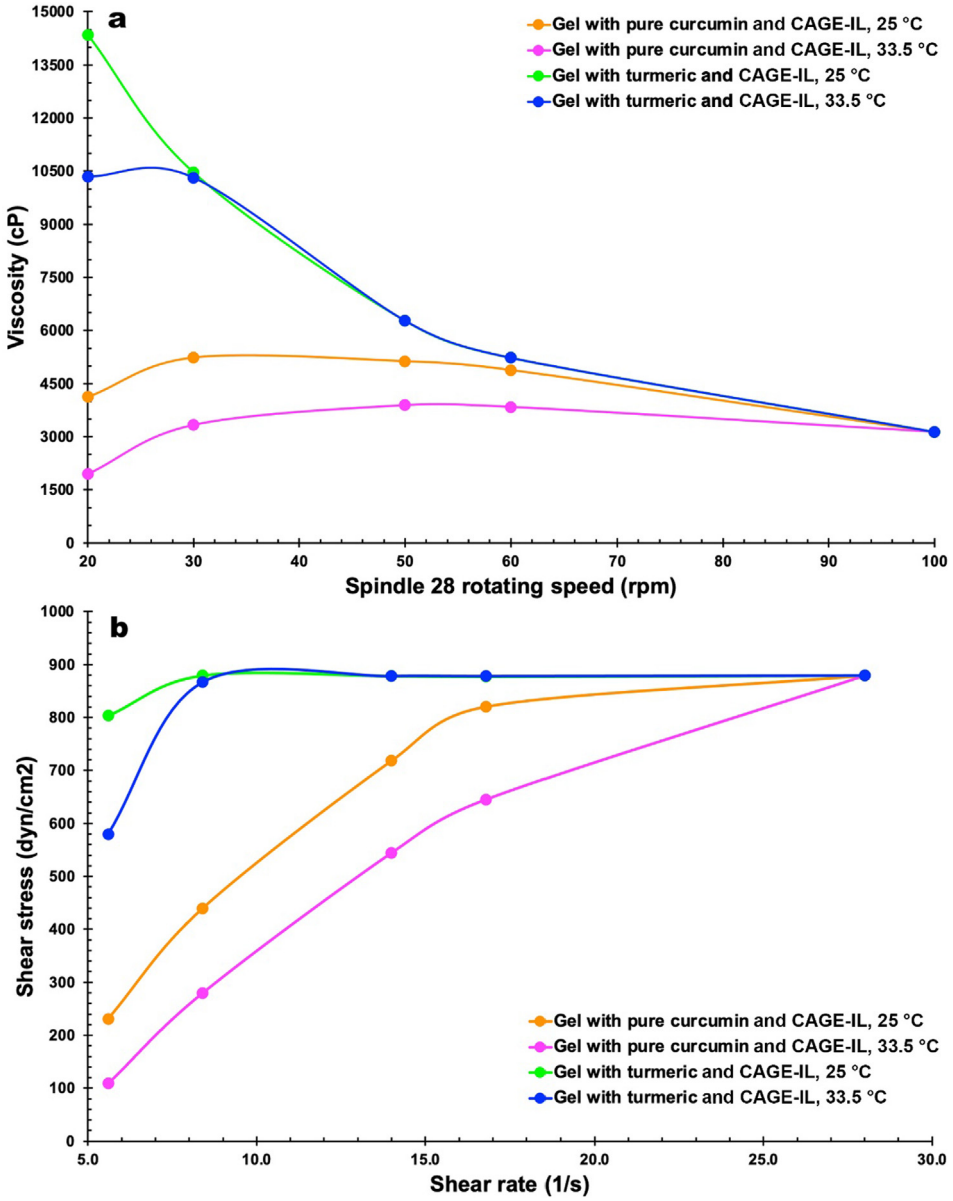

Fig. 10. Viscosity of the gel formulations integrating CAGE-IL and either pure curcumin or commercial turmeric for two different temperatures, viz. 25 °C and 33.5 °C (a) and relationship between shear stress and shear rate (b).

the employed vehicle may also favor its permeation, a conclusion that apparently seem to explain the higher amount of permeated curcumin at higher levels of CAGE-IL in the research work described herein.

A careful inspection of the data displayed in Table 2 allows to conclude that the optimized gel formulation containing turmeric (integrating 2% (w/w) curcumin) and 2.0% (w/w) CAGE-IL allowed relatively high values for permeated curcumin (viz. $AUC_{0\text{-}12}$, $\mu g_{curcumin}$), curcumin permeation flow (viz. J, $\mu g_{curcumin}\ mm^{-2}_{skin}\ h^{-1}$) and curcumin permeation coefficient (viz. C_{max}, $\mu g\ mL^{-1}$), for a CAGE-IL concentration of 2.0% (w/w).

The analysis by infrared spectrophotometry with Fourier transform allows identification of functional groups present in a material. Each particular functional group absorbs at a characteristic frequency of radiation in the infrared spectrum, hence a plot of intensity versus frequency of radiation (infrared spectrum) allows to characterize the functional groups of a given material (Cienfuegos and Vaitsman, 2000). The FTIR analysis were carried out for samples of pure curcumin, commercial turmeric, gel formulation integrating pure curcumin, gel formulation integrating pure curcumin and CAGE-IL, and gel formulation integrating commercial turmeric and CAGE-IL (Fig. 9), to further elucidate the interaction of curcumin with LBG and CAGE-IL in the gel formulations. Curcumin showed its signature peaks at 1627.92 cm^{-1} (aromatic moiety C=C stretching and C=O bond stretching of the conjugated ketone), 1116.78 cm^{-1} (benzene ring stretching vibrations), 1508.33 cm^{-1} (C=O and C=C vibrations), 1456.26 cm^{-1} (attributable to the group —CH2), 1427.32 cm^{-1} (olefinic —CH_2 bending vibrations and stretch of the C=C bond of the aromatic and aliphatic ring), 1280.73 cm^{-1} (aromatic C—O of enol stretching vibrations), 1028.06 cm^{-1} (stretching vibrations of the bond C—O—C of the ether) (Yallapu et al., 2010; Chen et al. 2015; Darandale and Vavia, 2013; Gangwar et al., 2012; Li et al., 2015). The same exact peaks appear in the spectrum of commercial turmeric.

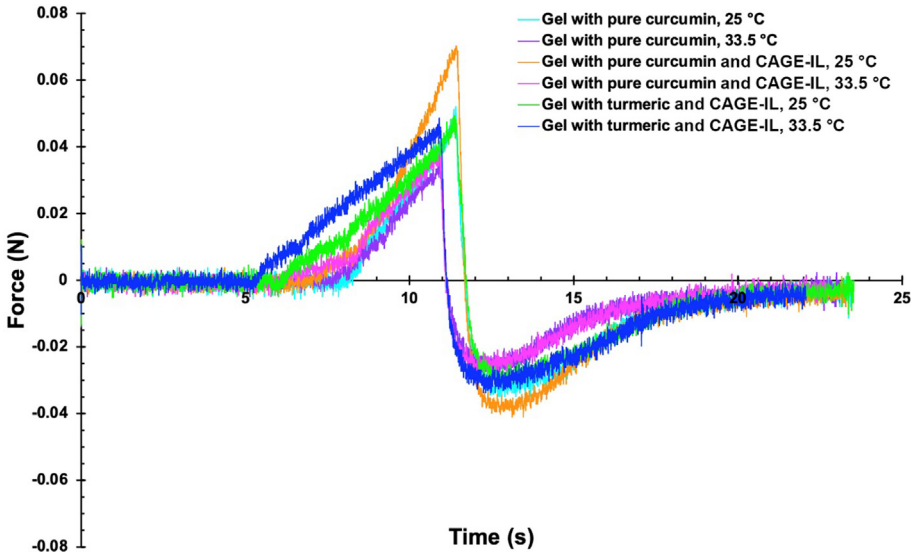

Fig. 11. Force-time curve of texture profile analysis of the gel formulations produced integrating pure curcumin with or without CAGE-IL and of the gel formulation integrating commercial turmeric and CAGE-IL, at 25 °C and 33.5 °C.

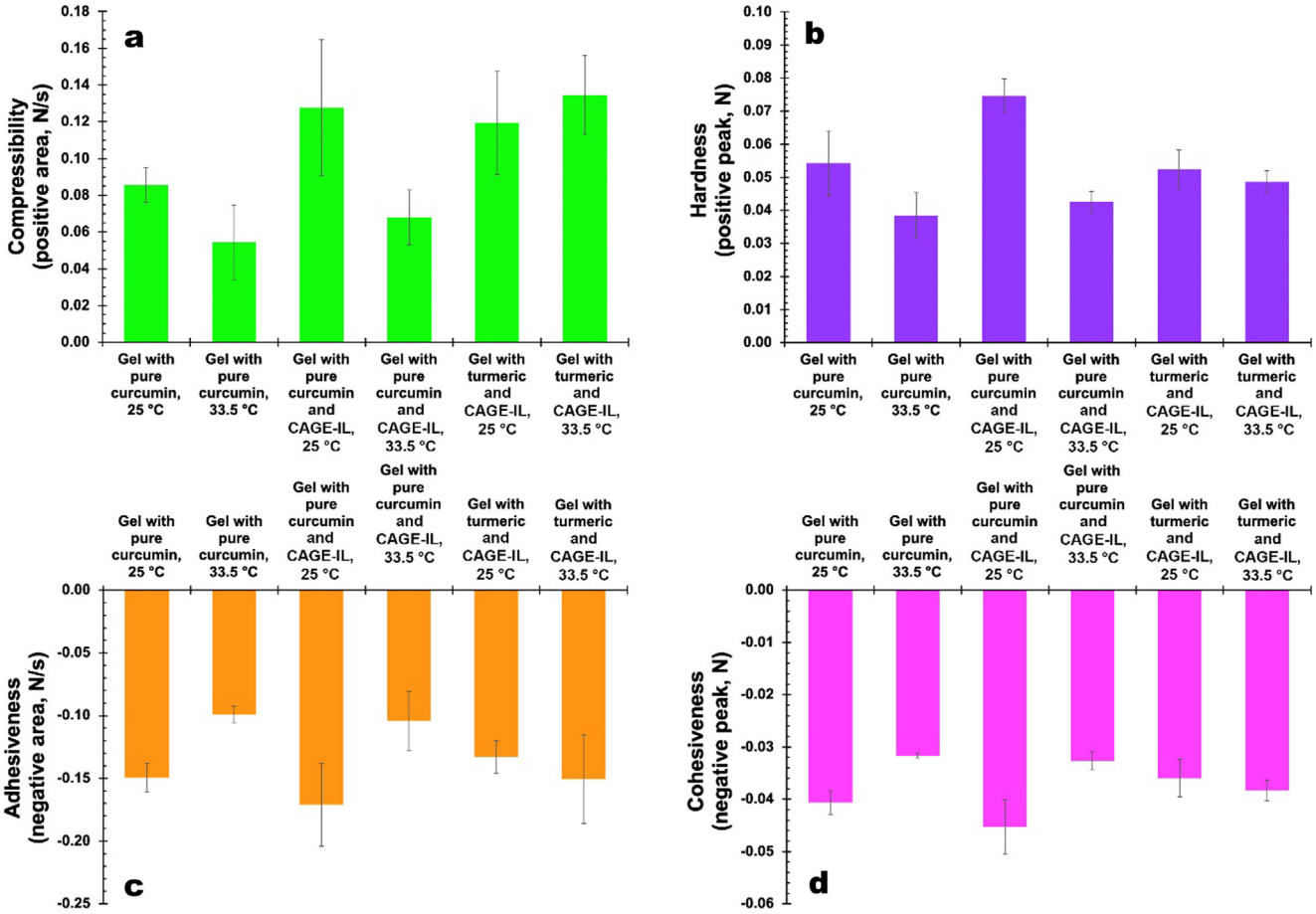

Fig. 12. Results obtained for the compressibility **(a)**, hardness **(b)**, adhesiveness **(c)** and cohesiveness **(d)** of the gel formulations produced integrating pure curcumin with or without CAGE-IL and of the gel formulation integrating commercial turmeric and CAGE-IL, at the two different temperatures assayed.

As observed in Fig. 9, the FTIR spectrum of curcumin indicates the presence of C—H bands at 713.66 cm^{-1}, 786.96 cm^{-1}, and 810.10 cm^{-1}, respectively. The peak at 1600.92 cm^{-1} corresponded to C=C stretching in the benzene ring. Moreover, the peak at 1508.33 cm^{-1} indicates the presence of ethylene group in curcumin (Nam et al., 2007). Additionally, the bands in the region of 962.48–810.10 cm^{-1} belonged to C—H out-of-plane bending and aromatic stretching.

The band around 1028.06 cm^{-1} is assigned to C—O stretching and a band at 1377.17 cm^{-1} is attributable to CH_2 scissoring vibra-

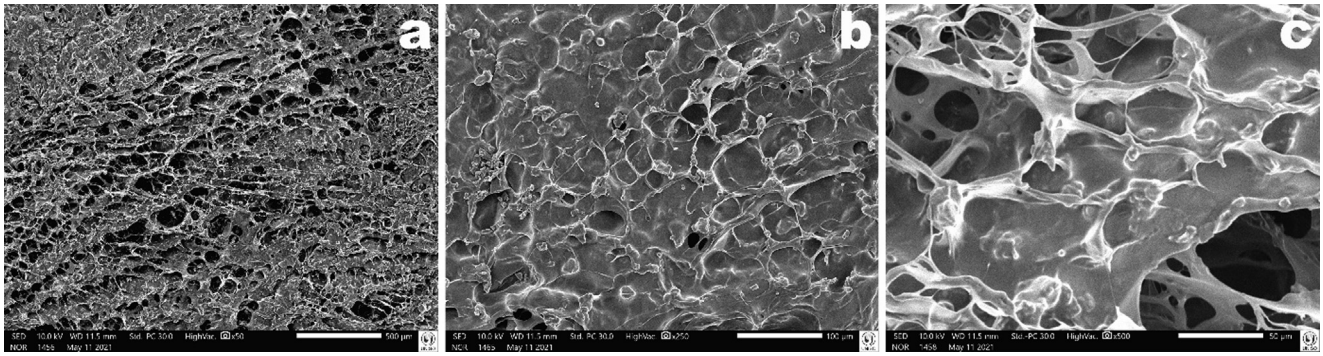

Fig. 13. Results obtained from the biopolysaccharide matrix morphology analysis of the optimized gel formulation via scanning electron microscopy at different magnifications, viz. x50 (a), x250 (b) and x500 (c).

tion in the component LBG of the gel formulations (Giri et al., 2015). Moreover, the bands in the region of 1350–1450 cm^{-1} show the symmetrical deformations of the CH_2 and COH groups in the LBG component of the gel formulations (Bashardoust et al., 2013).

The stretching bands and peaks of C—H at 713.66 cm^{-1}, 786.96 cm^{-1} and 810.10 cm^{-1}, —C—O— bands at 1602.85 cm^{-1} and 1629.85 cm^{-1}, and the ethylene group at 1510.26 cm^{-1} confirmed the presence of curcumin in our fabricated LBG/ CAGE-IL gels, a result that is in close agreement with previous findings by Virk et al. (2019) and Qiao and Duan (2020). The LBG gel formulations with curcumin exhibited peaks at 1629.85 cm^{-1} (aromatic moiety C=C stretching), 1602.85 cm^{-1} (benzene ring stretching vibrations) and 1510.26 cm^{-1} (C=O and C=C vibrations), which are the characteristic peaks of curcumin, indicating that curcumin retained its characteristics in the gel formulations.

The characteristic peaks of curcumin, LBG and CAGE-IL were present in the FTIR spectra of the gel formulations. It should be noted that in the spectrum of LBG-curcumin gels, the C=O stretching of Cur shifted from 1627.92 cm^{-1} to 1629.85 cm^{-1}; meanwhile, the C=C stretching in benzene ring at 1600.92 cm^{-1} and 1508.33 cm^{-1} was shifted to 1602.85 cm^{-1} and 1510.26 cm^{-1}, respectively. These results demonstrated that hydrogen bonding between LBG/ CAGE-IL and curcumin occurred in the gel formulations containing curcumin. In brief, LBG, CAGE-IL and Cur were compounded together excellently. These same types of interactions were reported by Qiao and Duan (2020).

Comparing the spectra of plain pure curcumin and commercial turmeric (Fig. 9) with the spectra of the gel formulations integrating curcumin and CAGE-IL, the same characteristic peaks can be observed with only minor variations in peak intensity, which clearly suggests that the chemical aspect of curcumin was preserved during incorporation into the biopolysaccharide gels.

While the results displayed in Fig. 9 suggest that the spectra of the gel formulations manifest themselves as a sum of the curcumin and LBG biopolymer spectra, indicating that no significative interaction occurred between curcumin, LBG and CAGE-IL, the FTIR spectra displayed in Fig. 9 indicates full compatibility between LBG, CAGE-IL and curcumin, with all the functional group frequencies being present.

The rheological characteristics of semi-solid products are important properties to be considered in the development of pharmaceutical formulations for topical use. Rheology has been a subject of great and growing importance for the cosmetic and pharmaceutical industries, as the rheological characteristics can influence the physical stability of the system, the spreadability, the sensory characteristics and the intended purposes of use. In the applied research work described here, gels prepared with concentrations of 2.5% (w/w) locust bean gum, 2.0% (w/w) CAGE-IL and 2.0% (w/w) of either pure curcumin or commercial turmeric were evaluated in terms of their viscosities at two different temperatures (25 °C (room temperature) and 33.5 °C (the normal average temperature of the human skin surface)). As can be observed from inspection of the data displayed in Fig. 10a, the gel formulations prepared with either pure curcumin or commercial turmeric exhibited quite different viscosities for low rotating speeds, irrespective of the temperature under scrutiny, with the former gel displaying much lower viscosity than the later. For higher rotating speeds of the spindle employed, both gel formulations exhibited the same viscosity irrespective of the temperature.

An inspection of the data displayed in Fig. 10a allows to conclude that both types of gel formulations displayed a non-linear plastic flow behavior. The gel formulation prepared with pure curcumin exhibiting a pseudoplastic (shear thinning) with yield (Herschel-Bulkley) behavior at both temperatures assayed, and the gel formulation prepared with commercial turmeric exhibiting a plastic behavior at both temperatures (Fig. 10b).

The compressibility, hardness, adhesiveness and cohesiveness of the gel formulations produced integrating pure curcumin with or without CAGE-IL and of the gel formulation integrating commercial turmeric and CAGE-IL, calculated from the force–time curves of texture profile analysis displayed in Fig. 11 for the two different temperatures assayed, viz. 25 °C and 33.5 °C. According to the results (Fig. 12), the best results in terms of (higher) compressibility and (lower) hardness were obtained at 33.5 °C for the gel prepared with CAGE-IL and commercial turmeric (Fig. 12a and b). At the temperature commonly encountered in the surface of the human skin, viz. 33.5 °C, the gel prepared with commercial turmeric also displayed the best results in terms of adhesiveness and cohesiveness (Fig. 12c and d). While "in-the-packaging" features such as lower compressibility and higher hardness together with lower adhesiveness and lower cohesiveness are desired at room temperature, those "out-of-the-packaging" features are better reversed at the intended temperature of use, viz. 33.5 °C, for skin applications. As can be observed from inspection of the data in Fig. 12, the gel that performed better in terms of these mechanical features was the one integrating CAGE-IL and commercial turmeric. The ability of the gel to stick on the surface of the skin is an especially important attribute, since its adhesiveness and cohesiveness are important characteristics for skin applications. These mechanical properties of the gels are mainly related with the biopolysaccharide's ability to form bonds in polymer chains, leading to resistance to their separation when subject to mechanical forces (Yang, 2012; Gong and Hong, 2012). In addition, the results obtained in the microstructural and morphological analysis of the gel matrix showed (Fig. 13) a highly porous and entangled network made of biopolysaccharide, which clearly favored release and availability of the entrapped curcumin for transdermal permeation aided by the CAGE-IL integrated in the formulation. The major goal

of the research work undertaken was to develop a gel formulation based on biopolysaccharides and integrating CAGE-IL and curcumin from commercial turmeric, suitable for application on the skin aiming at the delivery of curcumin via transdermal permeation. In our perspective, the gel applied directly to the skin should strongly adhere, allowing release of curcumin and easy removal of the spent gel from the skin by running water. Thus, compressibility, hardness, adhesiveness and cohesiveness were the mechanical resistance parameters evaluated, whereas resistance to traction, relaxation and resillience were not at all considered important in the research work developed.

5. Conclusions

In this research effort, the effect of CAGE-IL as a permeation enhancer of curcumin was studied, following abounding experimental evidence that this ionic liquid promotes transdermal permeation of bioactive macromolecules. The results of this study clearly show that the use of CAGE-IL highly enhances transdermal permeation of curcumin, with high potential in the treatment of skin diseases such as (but not limited to) psoriasis. The gel formulated with 2% (w/w) CAGE-IL and integrating 2% (w/w) of either pure curcumin or commercial turmeric allowed transdermal permeation of curcumin in reasonable amounts and concomitant skin retention of this bioactive molecule. The formulation integrating 2% (w/w) turmeric showed the best results in terms of mechanical properties, with a high potential for translation into “real world” applications with clear benefits to patients.

Declaration of Competing Interest

The authors declare that they have no known competing financial interests or personal relationships that could have appeared to influence the work reported in this paper.

Acknowledgements

Project funding by Fundação de Amparo à Pesquisa do Estado de São Paulo (FAPESP, São Paulo, Brazil) (FAPESP Refs. No. 2016/08884-3 (Project PneumoPhageColor) and 2016/12234-4 (Project TransAppIL)), is hereby gratefully acknowledged. Funding for Victor M. Balcão through a BPE grant from FAPESP (São Paulo, Brazil) (Ref. No. 2018/05522-9, Project PsaPhageKill) is hereby gratefully acknowledged. This work also received support from CNPq, National Council for Scientific and Technological Development Brazil, in the form of Research Productivity (PQ) fellowships granted to Victor M. Balcão (Refs. No. 306113/2014-7 and 308208/2017-0). The authors have no conflicts of interest whatsoever to declare.

References

Agrawal, S., Goel, R., 2016. Curcumin and its protective and therapeutic uses. Nati. J. Physiol. Pharm. Pharmacol. 6 (1), 1. https://doi.org/10.5455/njppp.10.5455/njppp.2016.6.3005201596.

Ahad, A., Raish, M., Jardan, Y.A.B., Al-Mohizea, A.M., Al-Jenoobi, F.I., 2021. Delivery of insulin via skin route for the management of diabetes mellitus: approaches for breaching the obstacles. Pharmaceutics 13 (100), 1–17.

Aiyalu, R., Govindarjan, A., Ramasamy, A., 2016. Formulation and evaluation of topical herbal gel for the treatment of arthritis in animal model. Braz. J. Pharm. Sci. 52 (3), 493–507.

Anindya, B., Anusree, R., Prosenjit, M., Tausif, A.M., 2015. Curcumin extraction : best solvent on the basis of spectrophotometric. Univers. J. Pharm. 4 (2), 48–52.

Arce, F., Asano, N., See, G.L., Oshizaki, T., Itakura, S., Todo, H., Sugibayashi, K., 2020. Prediction of skin permeation and concentration of rhododendrol applied as finite dose from complex cosmetic vehicles. Inter. J. Pharm. 578 (30), 186. https://doi.org/10.1016/j.ijpharm.2020.119186.

Banerjee, A., Ibsen, K., Iwao, Y., Zakrewsky, M., Mitragotri, S., 2017. Transdermal protein delivery using choline and geranate (cage) deep eutectic solvent. Adv. Healthc. Mater. 6 (15), 1601411. https://doi.org/10.1002/adhm.v6.1510.1002/adhm.201601411.

Bashardoust, N., Jenita, J.J.L., Zakeri–Milani, P., 2013. Physicochemical characterization and dissolution study of ibuprofen compression-coated tablets using locust bean gum. Dissolut. Technol. 20 (1), 38–43.

Boscariol, R., Caetano, É.A., Silva, E.C., Oliveira, T.J., Rosa-Castro, R.M., Vila, M.M.D.C., Balcão, V.M., 2021. Performance of choline geranate deep eutectic solvent as transdermal permeation enhancer: an in vitro skin histological study. Pharmaceutics 13 (4), 1–13. https://doi.org/10.3390/pharmaceutics13040540.

Burapan, S., Kim, M., Paisooksantivatana, Y., Eser, B.E., Han, J., 2020. Thai curcuma species: antioxidant and bioactive compounds. Foods 9 (9), 1–11.

Campos, W.F., Silva, E.C., Oliveira, T.J., Oliveira Jr, J.M., Tubino, M., Pereira, C., Vila, M. M.D.C., Balcão, V.M., 2020. Transdermal permeation of bacteriophage particles by choline oleate: potential for treatment of soft-tissue infections. Future Microbiol. 15 (10), 881–896. https://doi.org/10.2217/fmb-2019-0290.

Carvalho, D.M., Takeuchi, K.P., Geraldine, R.M., Moura, C.J., Torres, M.C.L., 2015. Production, solubility and antioxidant activity of curcumin nanosuspension. Food Sci. Technol 35 (1), 115–119.

Chen, X., Zou, L.-Q., Niu, J., Liu, W., Peng, S.-F., Liu, C.-M., 2015. The Stability, sustained release and cellular antioxidant activity of curcumin nanoliposomes. Molecules 20, 14293–14311. https://doi.org/10.3390/molecules200814293.

Chen, T., Guoping Lian, G., Kattou, P., 2016. *In silico* modelling of transdermal and systemic kinetics of topically applied solutes: model development and initial validation for transdermal nicotine. Pharmac. Res. 33 (7), 1602–1614. https://doi.org/10.1007/s11095-016-1900-x.

Cienfuegos, F., Vaitsman, D., 2000. Análise Instrumental [Instrumental Analysis]. Interciência, Rio de Janeiro, p. 2000.

Darandale, S.S., Vavia, P.R., 2013. Cyclodextrin-based nanosponges of curcumin: formulation and physicochemical characterization. J. Incl. Phenom. Macrocycl. Chem. 75 (3-4), 315–322.

Defraeye, T., Bahrami, F., Rossi, R. M., 2020. Inverse mechanistic modeling of transdermal drug delivery for fast identification of optimal model parameters. bioRxiv 2020.12.11.420836. https://doi.org/10.1101/2020.12.11.420836.

Dionísio, M., Grenha, A., 2012. Locust bean gum: exploring its potential for biopharmaceutical applications. J. Pharm. Bioallied Sci. 4 (3), 75–85.

EFSA (European Food Safety Authority), 2010. Scientific Opinion on the re-evaluation of curcumin (E 100) as a food additive. EFSA J. 8 (9), 1–46 https://efsa.onlinelibrary.wiley.com/doi/pdf/10.2903/j.efsa.2010.1679.

Egorova, K.S., Gordeev, E.G., Ananikov, V.P., 2017. Biological activity of ionic liquids and their application in pharmaceutics and medicine. Chem. Rev. 117 (10), 7132–7189.

Gangwar, R.K., Dhumale, V.A., Kumari, D., Nakate, U.T., Gosavi, S.W., Sharma, R.B., Kale, S.N., Datar, S., 2012. Conjugation of curcumin with PVP capped gold nanoparticles for improving bioavailability. Mater. Sci. Eng., C 32 (8), 2659–2663.

Gibrat, R., 1930. Une lois des repartitions économiques: l'effet proportionnel. Bull. STAT. 19, 469.

Giri, T.K., Pure, S., Tripathi, D.K., 2015. Synthesis of graft copolymers of acrylamide for locust bean gum using microwave energy: swelling behavior, flocculation characteristics and acute toxicity study. Polímeros 25 (2), 168–174. https://doi.org/10.1590/0104-1428.1717.

Gong, J.P., Hong, W., 2012. Mechanics and physics of hydrogels. Soft Matter 8, 8006–8007.

Guimaraes, A.F., Vinhas, A.C.A., Gomes, A.F., Souza, L.H., Krepsky, P.B., 2020. Essential oil of curcuma longa l. rhizomes chemical composition, yield variation and stability. Quím. Nova 43 (7), 909–913.

Harada, L.K., Pereira, J.F.B., Campos, W.F., Silva, E.C., Moutinho, C.G., Vila, M.M.D.C., Oliveira, J.M., Teixeira, J.A., Balcão, V.M., Tubino, M., 2018. Insights into protein-ionic liquid interactions aiming at macromolecule delivery systems. J. Braz. Chem. Soc. 29, 1983–1998. https://doi.org/10.21577/0103-5053.20180141.

Hassanzadeh, K., Buccarello, L., Dragotto, J., Mohammadi, A., Corbo, M., Feligioni, M., 2020. Obstacles against the marketing of curcumin as a drug. Int. J. Mol. Sci. 21 (18), 1–35.

Hernandes, A.N., Boscariol, R., Balcão, V.M., Vila, M.M.D.C., 2021. Transdermal permeation of caffeine aided by ionic liquids: Potential for enhanced treatment of cellulite. AAPS PharmSciTech 22, 121. https://doi.org/10.1208/s12249-021-01956-5.

Hewlings, S.J., Kalman, D.S., 2017. Curcumin: A review of its' effects on human health. Foods 6 (10), 92. https://doi.org/10.3390/foods6100092.

Islam, M.R., Chowdhury, R., Wakabayashi, R., Kamiya, N., Moniruzzaman, M., Goto, M., 2020. Ionic liquid-in-oil microemulsions prepared with biocompatible choline carboxylic acids for improving the transdermal delivery of a sparingly soluble drug. Pharmaceutics 12 (4), 1–18.

Jantarat, C., Sirathanarun, P., Boonmee, S., Meechoosin, W., Wangpittaya, H., 2018. Effect of piperine on skin permeation of curcumin from a bacterially derived cellulose-composite double-layer membrane for transdermal curcumin delivery. Sci. Pharm. 86 (39), 1–14. https://doi.org/10.3390/scipharm86030039.

Jorge, L.R., Harada, L.K., Silva, E.C., Campos, W.F., Moreli, F.C., Shimamoto, G., Pereira, J.F.B., Oliveira Jr., J.M., Tubino, M., Vila, M.M.D.C., Balcão, V.M., 2020. Non-

invasive transdermal delivery of human insulin using ionic liquids: in vitro studies. Front. Pharmacol. 11, 1–17.
Khalid, S., Rizwan, B., Aslam, M., Sharmeen, Z., Zubair, R., Arif, A., Mahmood, S., Fatima, M., 2020. Therapeutic potential of curcumin in *Curcuma longa* : a review. Merit Res. J. Food Sci. Technol. 5 (3), 32–41.
Kim, L., Lio, P., 2020. Turmeric, curcumin, and curcuminoids: a dermatologic review. Clinical Focus., 38–42
Ko, J., Mandal, A., Dhawan, S., Shevachman, M., Mitragotri, S., Joshi, N., 2021. Clinical translation of choline and geranic acid deep eutectic solvent. Bioeng. Transl. Med. 6 (2). https://doi.org/10.1002/btm2.10191.
Kocaadam, B., Şanlier, N., 2017. Curcumin, an active component of turmeric (*Curcuma longa*), and its effects on health. Crit. Ver. Food Sci. Nutr. 57 (13), 2889–2895.
Kováčik, A., Kopečná, M., Vávrová, K., 2020. Permeation enhancers in transdermal drug delivery: benefits and limitations. Expert Opin. Drug Deliv. 17 (2), 145–155.
LaCount, T.D., Zang, Q., Hao, J., Ghosh, P., Raney, S.G., Talattof, A., Kasting, G.B., Kevin Li, S., 2020. Modeling temperature-dependent dermal absorption and clearance for transdermal and topical drug applications. AAPS J. 22 (3), 70. https://doi.org/10.1208/s12248-020-00451-2.
Li, J., Lee, I.W., Shin, G.H., Chen, X., Park, H.J., 2015. Curcumin-Eudragit® E PO solid dispersion: a simple and potent method to solve the problems of curcumin. Eur. J. Pharm. Biopharm. 94, 322–332.
Limpert, E., Stahel, W.A., Abbt, M., 2001. Log-normal Distributions across the Sciences: Keys and Clues: on the charms of statistics, and how mechanical models resembling gambling machines offer a link to a handy way to characterize log-normal distributions, which can provide deeper insight into variability and probability—normal or log-normal: that is the question. Bioscience 51 (5), 341–352. https://doi.org/10.1641/0006-3568(2001)051[0341:LNDATS]2.0.CO;2.
Mohammadinejad, R., Kumar, A., Ranjbar-Mohammadi, M., Ashrafizadeh, M., Han, S. S., Khang, G., Roveimiab, Z., 2020. Recent advances in natural gum-based biomaterials for tissue engineering and regenerative medicine: a review. Polymers 12 (176), 1–38.
Mitragotri, S., Anissimov, Y.G., Bunge, A.L., Frasch, H.F., Guy, R.H., Hadgraft, J., Kasting, G.B., Lane, M.E., Roberts, M.S., 2011. Mathematical models of skin permeability: an overview. Int. J. Pharm.v. 418 (1), 115–129.
Mitzenmacher, M., 2003. A brief history for generative models for power law and lognormal distributions. Int. Math. 1 (2), 226–251.
Musiał, M., Zorębski, E., Malarz, K., Kuczak, M., Mrozek-Wilczkiewicz, A., Jacquemin, J., Dzida, M., 2021. Cytotoxicity of ionic liquids on normal human dermal fibroblasts in the context of their present and future applications. ACS Sustain. Chem. Eng. 9 (22), 7649–7657.
Nam, S.H., Nam, H.Y., Joo, J.R., Baek, I.S., Park, J., 2007. Curcumin-loaded PLGA nanoparticles coating onto metal stent by electrophoretic deposition techniques. Bull. Korean Chem. Soc. 28, 397–402.
Nelson, K.M., Dahlin, J.L., Bisson, J., Graham, J., Pauli, G.F., Walters, M.A., 2017. The essential medicinal chemistry of curcumin. J. Med. Chem. 60 (5), 1620–1637.
Nikolic, I., Mitsou, M., Pantelic, I., Randjelovic, D., Markovic, B., Papadimitriou, V., Xenakis, A., Lunter, D.J., Zugic, A., Savic, S., 2020. Microstructure and biopharmaceutical performances of curcumin-loaded low-energy nanoemulsions containing eucalyptol and pinene: Terpenes' role overcome penetration enhancement effect? Eur. J. Pharm. Sci. 142 (15), 105–135.
Panahi, Y., Fazlolahzadeh, O., Atkin, S.L., Majeed, M., Butler, A.E., Johnston, T.P., Sahebkar, A., 2019. Evidence of curcumin and curcumin analogue effects in skin diseases: a narrative review. J. Cell. Physiol. 234 (2), 1165–1178.
Pasqui, D., De Cagna, M., Barbucci, R., 2012. Polysaccharide-based hydrogels: the key role of water in affecting mechanical properties. Polymers 4 (3), 1517–1534.
Patel, N.A., Patel, N.J., Patel, R.P., 2009. Formulation and evaluation of curcumin gel for topical application. Pharm. Dev. Technol. 14 (1), 83–92.
Pettinelli, N., Rodríguez-Llamazares, S., Farrag, Y., Bouza, R., Barral, L., Feijoo-Bandín, S., Lago, F., 2020. Poly(hydroxybutyrate-co-hydroxyvalerate) microparticles embedded in κ-carrageenan/locust bean gum hydrogel as a dual drug delivery carrier. Int. J. Biol. Macromol. 146, 110–118.
Pradal, J., 2020. Comparison of Skin permeation and putative anti-inflammatory activity of commercially available topical products containing ibuprofen and diclofenac. J. Pain Res. 13, 2805–2814.
Purushothaman, S., Cama, J., Keyser, U.F., 2016. Dependence of norfloxacin diffusion across bilayers on lipid composition. Soft Matter 12 (7), 2135–2144.
Pusnik, M., Imeri, M., Deppierraz, G., Bruinink, A., Zinn, M., 2016. The agar diffusion scratch assay – a novel method to assess the bioactive and cytotoxic potential of new materials and compounds. Sci. Rep. 6, 1–10. https://doi.org/10.1038/srep20854.
Qiao, Y., Duan, L., 2020. Curcumin-loaded polyvinyl butyral film with antibacterial activity. e-Polymers 20 (1), 673–681.
Rendon, A., Schäkel, K., 2019. Psoriasis pathogenesis and treatment. Int. J. Mol. Sci. 20 (6), 1475. https://doi.org/10.3390/ijms20061475.
Rocha, L.K.H., Favaro, L.I.L., Rios, A.C., Silva, E.C., Silva, W.F., Stigliani, T.P., Guilger, M., Lima, R., Oliveira, J.M., Aranha, N., Tubino, M., Vila, M.M.D.C., Balcão, V.M., 2017. Sericin from Bombyx mori cocoons. Part I: Extraction and physicochemical-biological characterization for biopharmaceutical applications. Process Biochem. 61, 163–177. https://doi.org/10.1016/j.procbio.2017.06.019.
Rogero, S.O., Lugão, A.B., Ikeda, T.I., Cruz, Á.S., 2003. Teste in vitro de citotoxicidade: estudo comparativo entre duas metodologias [In vitro cytotoxicity test: comparative study between two methodologies]. Mat. Res. 6 (3), 317–320. https://doi.org/10.1590/S1516-14392003000300003.
Salerno, C., Carlucci, A.M., Bregni, C., 2010. Study of in vitro drug release and percutaneous absorption of fluconazole from topical dosage forms. AAPS PharmSciTech 11 (2), 986–993. https://doi.org/10.1208/s12249-010-9457-1.
Sato, M.E.O., Gomara, F., Pontarolo, R., Andreazza, I.F., Zaroni, M., 2007. Permeação cutânea *in vitro* do ácido kójico. Braz. J. Pharm Sci 4 (2), 195–203.
Selvadurai, P.A., Selvadurai, A.P.S., 2014. On the effective permeability of a heterogeneous porous medium: the role of the geometric mean. Philos. Mag. Part A: Mater. Sci. 94 (20), 2318–2338. https://doi.org/10.1080/14786435.2014.913111.
Shevachman, M., Mandal, A., Mitragotri, S., Joshi, N., 2020. A long-lasting sanitizing skin protectant based on cage, a choline and geranic acid eutectic. MedRxiv 7, 1–14. https://doi.org/10.1101/2020.08.04.20161067.
Sidat, Z., Marimuthu, T., Kumar, P., du Toit, L.C., Kondiah, P.P.D., Choonara, Y.E., Pillay, V., 2019. Ionic liquids as potential and synergistic permeation enhancers for transdermal drug delivery. Pharmaceutics 11, 96. https://doi.org/10.3390/pharmaceutics11020096.
Siddiqui, N.A.L., 2015. Evaluation of thermo sensitivity of curcumin and quantification of ferulic acid and vanillin as degradation products by a validated HPTLC method. Pak. J. Pharm. Sci. 28 (1), 299–305.
Silva, E.C., Oliveira, T.J., Moreli, F.C., Harada, L.K., Vila, M.M.D.C., Balcão, V., 2021. Newly isolated lytic bacteriophages for *Staphylococcus intermedius*, structurally and functionally stabilized in a hydroxyethylcellulose gel containing choline geranate: potential for transdermal permeation in veterinary phage therapy. Res. Vet. Sci. 24 (135), 42–58.
Singh, A., Avupati, V.R., 2017. Development and validation of UV-spectrophotometric method for the estimation of curcumin in standardised polyherbal formulations. J. Young Pharm. 9 (4), 491–495.
Stohs, S.J., Chen, O., Ray, S.D., Ji, J., Bucci, L.R., Preuss, H.G., 2020. Highly bioavailable forms of curcumin and promising avenues for curcumin-based research and application: a review. Molecules 25 (1397), 1–12.
Todo, H., 2017. Transdermal permeation of drugs in various animal species. Pharmaceutics 9 (3), 1–11.
Virk, R.S., Rehman, M.A.U., Munawar, M.A., Schubert, D.W., Goldmann, W.H., Dusza, J., Boccaccini, A.R., 2019. Curcumin-containing orthopedic implant coatings deposited on poly-ether-ether-ketone/bioactive glass/hexagonal boron nitride layers by electrophoretic deposition. Coatings 9, 572. https://doi.org/10.3390/coatings9090572.
Vollono, V., Mattia, F., Roberta, G., Federico, I., Emi, D., Chiara, T., Luca, B., Campione, E., 2019. Potential of curcumin in skin disorders. Nutrients 11 (2169), 1–25.
Williams, A.C., Cornwell, P.A., Barry, B.W., 1992. On the non-gaussian distribution of human skin permeabilities. Int. J. Pharm. 86 (1), 69–77. https://doi.org/10.1016/0378-5173(92)90032-W.
Yallapu, M.M., Jaggi, M., Chauhan, S.C., 2010. β-Cyclodextrin-curcumin self-assembly enhances curcumin delivery in prostate cancer cells. Colloids Surf. B 79 (1), 113–125.
Yang, T., 2012. Mechanical and swelling properties of hydrogels, KTH Ytbehandlingsteknik, Doctoral thesis, p. 77. Available from http://www.diva-portal.org/smash/get/diva2:571374/FULLTEXT01.pdf.
Yoo, B., Jing, B., Jones, S.E., Lamberti, G.A., Zhu, Y., Shah, J.K., 2016. Molecular mechanisms of ionic liquid cytotoxicity probed by an integrated experimental and computational approach. Sci. Rep. 6 (19889), 1–7. https://doi.org/10.1038/srep19889.
Yousef, S.A., Mohammed, Y.H., Namjoshi, S., Grice, J.E., Benson, H.A.E., Sakran, W., Roberts, M.S., usef et al.,. Mechanistic evaluation of enhanced curcumin delivery through human skin in vitro from optimised nanoemulsion formulations fabricated with different penetration enhancers. Pharmaceutics 11 (639), 1–20. https://doi.org/10.3390/pharmaceutics11120639.
Zakrewsky, M., Banerjee, A., Apte, S., Kern, T.L., Jones, M.R., Sesto, R.E.D., Koppisch, A. T., Fox, D.T., Mitragotri, S., 2016. Choline and geranate deep eutectic solvent as a broad-spectrum antiseptic agent for preventive and therapeutic applications. Adv. Healthc. Mater. 5 (11), 1282–1289.
Zakrewsky, M., Lovejoy, K.S., Kern, T.L., Miller, T.E., Le, V., Nagy, A., Goumas, A.M., Iyer, R.S., Del Sesto, R.E., Koppisch, A.T., Fox, D.T., Mitragotri, S., 2014. Ionic liquids as a class of materials for transdermal delivery and pathogen neutralization. PNAS 111 (37), 13313–13318.
Zhang, Y., Lane, M.E., Moore, D.J., 2020. An investigation of the influence of PEG 400 and PEG-6-caprylic/capric glycerides on dermal delivery of niacinamide. Polymers 12 (2907), 1–11.
Zhu, T., Mao, J., Cheng, Y., Liu, H., Lv, L.u., Ge, M., Li, S., Huang, J., Chen, Z., Li, H., Yang, L., Lai, Y., 2019. Recent progress of polysaccharide-based hydrogel interfaces for wound healing and tissue engineering. Adv. Mater. Interfaces 6 (17), 1900761. https://doi.org/10.1002/admi.v6.1710.1002/admi.201900761.